School of Engineering and Digital Arts

University of Kent

EENG6000: Project

Deployment of Reconfigurable Intelligent Surfaces

by

Huy Viet Le

hvl3

Supervisor: Dr Huiling Zhu

6th April 2023

Submitted to the School of Engineering and Digital Arts as a part of the requirements for the degree of Bachelor of Electronic and Computer Engineering.

Declaration

I certify that I have read and understood the entry in the School Student Handbook on Plagiarism and Duplication of Materials, and that all material in this assignment is my own work, except where I have indicated appropriate references.

Signed: 

Date:_____06/04/2023_____

Acknowledgements

I would like to express my utmost gratitude to Dr Huiling Zhu, whose supervision, guidance and insights into the field of communication systems she provided me throughout my studies have made me a much better engineer and played a large part in the completion of this challenging, yet also interesting, rewarding, and fulfilling project. Special thanks also belong to the University of Kent PhD candidates Umar Bin Mohd Fayzak and Mahdi Eskandari who have assisted me profoundly throughout the project every time I needed to fill the gap in my understandings. I would like to thank my course mate and friend Junqi Liu who shared my struggles conducting a project in the same field of research and has been an invaluable source of both moral and academic support.

Lastly, I would like to express my greatest and eternal gratitude to my parents, Huy Duong Le and Thi Yen Pham and siblings, Huy Dat Le and Thao An Le, who have always been surrounding me with love and support and who are and always will be the motivation behind all my efforts.

Abstract

This dissertation investigates the potential advantages of using Reconfigurable Intelligent Surfaces (RIS) in wireless communication systems. The main objective is to evaluate the performance of a system model that incorporates RIS to control the wireless channel using universal parameters like bit-error ratio (BER), signal-to-noise ratio (SNR), data rate, and outage probability. The simulations are conducted using MATLAB software, which allows for flexibility in modifying the system model.

The dissertation explores the impact of RIS on communication systems that have single and multi-antenna transmitter and receiver devices. It considers the placement of RIS, the number of elements within the surface, or the displacement of receivers. The system is also evaluated for a multi-user scenario. The results are compared with conventional SISO, MISO, SIMO, and MIMO systems. The performance improvement for each communications system model is discussed based on the simulations.

RIS is considered a revolutionary technology in the field of wireless communication, and it is planned to be one of the main building blocks of future 6G networks. RIS can enable more reliable cellular service, higher transfer rates, and better interconnectivity between devices. The dissertation aims to contribute to ongoing research efforts on RIS technology and its implementation into future 6G network structure.

The dissertation evaluates the impact of RIS on communication systems by considering the ability of RIS to steer incoming signals towards the receiver and decrease the impact of a hostile channel environment, especially in a MIMO system where it contributes to signal diversity and better multiplexing. It also evaluates changes in performance of a RIS-assisted channel with different configurations, such as changing numbers of transmitting and receiving antennas, the number of RIS elements deployed and their displacement in the scenario setting, the number of users, and the effect of RIS on different precoding schemes.

In conclusion, this dissertation proposes a system model that incorporates RIS to control the wireless channel and evaluates its performance using universal parameters. It investigates the impact of RIS on communication systems with different configurations and provides a full performance evaluation and analysis of a RIS-assisted communications system. The results are compared with conventional systems, and the proposed setting based on acquired data and previous work contributes to ongoing research efforts on RIS technology in future 6G networks.

Contents

Declaration 1

Acknowledgements 2

Abstract 3

List of Abbreviations 8

1 Introduction 9

1.1 Motivation 9

1.2 Project Overview 9

1.2.1 Aims and Objectives 9

1.2.2 Deliverables 10

2 Literature Review 11

2.1 Communications System 11

2.1.1 Modulation and Demodulation 12

2.1.1.1 Quadrature Amplitude Modulation (QAM) 12

2.1.1.2 Phase Modulation (PM) 13

2.1.2 Large-Scale Fading 13

2.1.2.1 Path Loss 14

2.1.2.2 Shadowing 14

2.1.3 Small-Scale Fading 15

2.1.3.1 Rayleigh Fading 15

2.1.3.2 Rician Fading 16

2.2 Multiple Input Multiple Output System (MIMO) 16

2.2.1 Diversity 17

2.2.2 Multiplexing 18

2.2.3 Precoding 19

2.2.3.1 Zero-forcing (ZF) 19

2.2.3.2 Block Diagonalization (BD) 20

2.3 RIS Concept 21
2.3.1 Types of RIS 22
2.3.2 Limitations 22
2.3.2.1 Channel State Information (CSI) 22
2.3.2.2 Near-field Characteristics 23
2.3.2.3 Mutual Coupling 23
3 System Specification 24
3.1 System Overview 24
3.2 Coordinate System 25
3.2.1 Euclidean Distance 25
3.2.2 Departure Angle and Path loss 26
3.3 Impedance Patterns and Correlation 27
3.4 Precoding 28
3.4.1 Zero-forcing 28
3.4.2 Block Diagonalization 29
3.5 Channel Model 30
4 Implementation 32
4.1 Element Positioning 32
4.2 Distance and Angle Calculations 33
4.3 Signal Data Generation 33
4.4 Modulation 33
4.5 Path Loss 33
4.6 Channel Model Implementation 34
4.6.1 Correlation 34
4.6.2 Precoding 34
4.6.2.1 Zero-forcing 34
4.6.2.2 Block Diagonalization 35

4.7 Performance Evaluation Criteria 35
4.7.1 Signal to Noise Ratio (SNR) 35
4.7.2 Bit Error Rate (BER) 36
4.7.3 Outage Probability 36
4.7.4 Data Rate 36
5 Results 36
5.1 Single-User Scenario 37
5.2 Multi-User Scenario 41
4.3. Overall Results 42
6 Project Management 43
6.1 Project Plan 43
6.2 Budget and Communication 44
6.3 Risk Assessment 44
7 Conclusions and Future Work 45
7.1 Conclusions 45
7.2 Future Work 45
7.2.1 Channel -State Information (CSI) 45
7.2.2 Moving Receiver 45
References 46
APPENDIX A 52
Revised Gantt Chart 52
APPENDIX B 52
Original Gantt Chart 52
APPENDIX C 53
Channel Generation 53
APPENDIX D 54
Multi-User 54

APPENDIX E 58
Single-User 58
APPENDIX F 61

List of Abbreviations

Abbreviation	**Meaning**
BS	Base Station
UE	User Equipment
MIMO	Multiple Input Multiple Output
RIS	Reconfigurable Intelligent Surface
BER	Bit-Error Ratio
SNR	Signal-to-Noise Ratio
SISO	Single Input Single Output
SIMO	Single Input Multiple Output
MISO	Multiple Input Single Output
CSI	Channel State Information
CSIT	Channel Side Information at the Transmitter
CSIR	Channel Side Information at the Receiver
BD	Block Diagonalization
ZF	Zero-Forcing
PM	Phase modulation
PSK	Phase-Shift Keying
DPSK	Differential Phase-Shift Keying
OPSK	Offset Phase-Shift Keying
CPFSK	Continuous-Phase Frequency-Shift Keying
QAM	Quadrature Amplitude Modulation
LOS	Line-of-Sight
EQC	Equal Gain Combining
SVD	Singular Value Decomposition
AWGN	Additive White Gaussian Noise
EQ	Equalizer

1 Introduction

Reconfigurable Intelligent Surface refers to a planar surface, a two-dimensional array of closely spaced less than half wavelength-sized scatterer elements capable of reflecting incident electromagnetic waves to a predetermined receiver position [1]. The properties of reflection are modifiable and the modifications are meant to be controllable by real-time programming . The surface can be mounted on walls, buildings, vehicles, boards etc. in both indoor and outdoor environments. If RIS are employed within a wireless communications system and placed strategically in the space between the transmitter and the receiver, the characteristics of the wireless channel can be improved significantly by allowing channel control which has not been possible before the arrival of RIS [2].

1.1 Motivation

Current-generation communication network systems have relied on improvements made through the implementation of newest technologies on both the transmitter and the receiver side while considering the channel link as an uncontrollable object with uncertain reliability. While exploitation of the spatial domain and multiplexing attributes in MIMO systems have significantly assisted to achieve higher diversity and thus reliability and transfer rates of current communications network, due to the rapidly increasing global demand for data transfers, current technology has been moving towards higher frequency bands to satisfy the supply and demand of global data communications. However, the unreliability concern increases with higher frequency bands being exploited for use due to even higher uncontrollability [1]. However, RIS with its capability to steer the incoming signal toward the receiver can decrease the impact of the hostile channel environment. The impact of RIS is further impressive within a MIMO system where it contributes to system's signal diversity allowing better multiplexing.

1.2 Project Overview

The project aims to simulate and evaluate the effects of a RIS-assisted controllable channel on the performance of the communications link within different scenarios and use cases. This is conducted through a set of specifically designed MATLAB simulations of both currently system models and communication systems and improved models with RIS deployed in the environment.

1.2.1 Aims and Objectives

As the RIS technology is still in its initial stages of testing, an elaborate and detailed set of simulations and testing needs to be executed to investigate the actual performance, viability of

implementation, and worth over conventional transmission technologies. These aspects can vary significantly depending on the use case, deployment environment and scenario. The RIS-assisted system is simulated in different scenarios and in different use cases thanks to the MATLAB simulation tool developed being robust enough to simulate the system and generate channels with modifiable number of users, antennas per user, precoding schemes, varying sizes and locations of system components and their sub-components. The performance will be assessed based on objective parameters of bit error rate (BER), signal to noise and ratio (SNR), outage probability, and data rate. The objectives of the projects are the following:

- Introduce and present the concept of RIS and theoretical background.
- Present the potential advantages of RIS deployment.
- Background research of existing RIS-assisted channel models
- Simulation of the RIS-assisted channel model in a given scenario to investigate the performance of the system compared to the conventional channel.

1.2.2 Deliverables

The dissertation provides a full analysis and evaluation of the performance and advantages of the use of RIS within a communications system. A discussion over the worth and the best use case for the technology will be conducted. Along with the dissertation a fully functional bespoke MATLAB-based simulation tool developed to achieve the objectives of the project will be provided for review.

2 Literature Review

The literature review provides a good source for understanding the topic of the dissertation and related fields of study and expertise. The topic of research of this dissertation is communications system performance analysis and evaluation with a focus on the deployment of RIS. To acquire a sufficiently robust amount of knowledge and data on conventional communication systems and channel characteristics models and to better understand the concept of RIS, a thorough background research of the work that has been done in the field of RIS research and development needs to be carried out. The main portals used for the background research are Google Scholar and IEEE Xplore®. Through the background research, currently developed concepts and models can be better understood from different perspectives and concerns and limitations of the technology discussed can be identified. From there new ideas and concrete directions for further research and for focus of this project can be developed.

2.1 Communications System

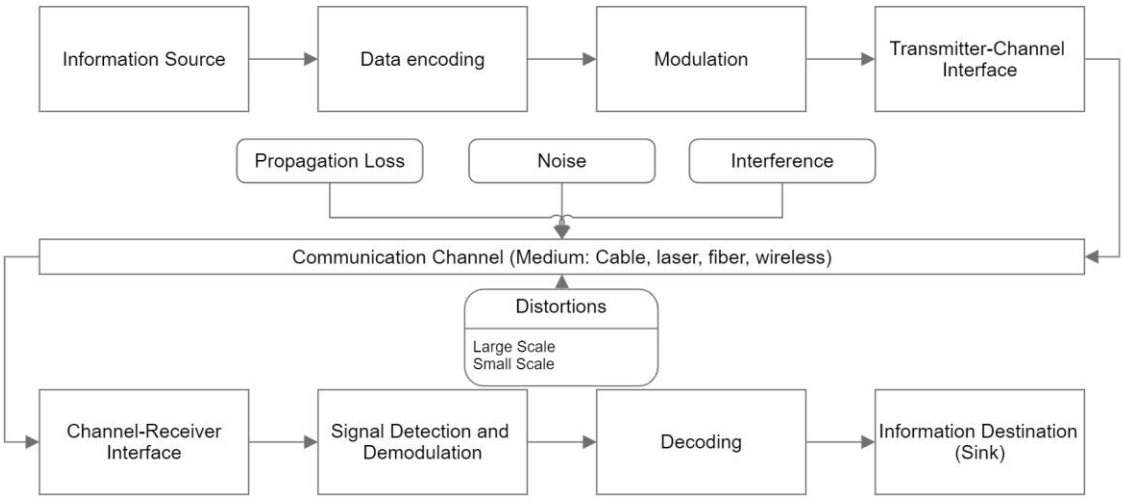

Figure 2.1: Basic Communications System Block Diagram

Figure 2.1 shows a generalized model of a communications system. The information source is encoded to be transmitted and goes through line coding or modulation based on whether the transmission is analogue or digital respectively. The signal is then sent through the channel by mixing with a pre-generated carrier signal at the transmitter side. At the receiver, the signal is demodulated and decoded to retrieve the received data. However, the signal is corrupted by various kinds of distortions, including large and small scale fading and interference from other surrounding devices [4].

2.1.1 Modulation and Demodulation

Consider a bandpass cosine wave given by Equation 2.1:

$$s(t) = Acos(2\pi ft + \phi) \quad (2.1.)$$

where

A - the wave amplitude

f - the wave frequency

ϕ - is the phase of the wave.

Modulation is described as the impartation of information onto electromagnetic (EM) waves. This can be done by arranging one or more of the following parameters of the wave: amplitude, frequency, and phase. The cosine wave given by Equation 2.1, or any other waveform, can also be expressed by Equation 2.2:

$$s(t) = Re\{g(t)e^{j2\pi f_c t}\} \quad (2.2.)$$

where

$g(t)$ - complex envelope of $s(t)$, which is the baseband equivalent of $s(t)$.

Modulation is the process of encoding the source information $m(t)$ into a bandpass signal $s(t)$. The complex envelope $g(t)$ is a function of the modulating signal $m(t)$, thus $g(t) = g[m(t)]$ which performs the mapping operation on $m(t)$. The mapping function depends on the modulation scheme chosen [2].

Digital Modulation encodes a symbol consisting of a definite number of data bits into one of the several possible transmitted signals [1]. By having a predetermined set of symbols, the probability of error detection is minimized at the receiving end as the receiver can decode the signal by comparison of the signal data with the closest possible symbols. Digital modulation schemes can be divided into four categories: Amplitude Shift Keying (ASK), Quadrature Amplitude Modulation, Phase Modulation, or Continuous Phase Modulation [4].

2.1.1.1 Quadrature Amplitude Modulation (QAM)

QAM is a digital modulation technique that combines amplitude and phase modulation to transmit digital data over a communication channel. In QAM, the modulating signal is a digital signal that is split into two components: an in-phase (I) component and a quadrature (Q) component, the real and imaginary parts of $g(t)$ are placed on a rectangular trellis. In QAM modulation, the amplitude and phase of the carrier signal are modulated by the I and Q components of the modulating signal. This results in a modulated signal that has varying amplitude and phase, which can be used to represent digital data. The QAM modulated signal

can be visualized as a constellation diagram, which plots the I and Q components of the modulating signal on a graph. Symbols mapped using the QAM scheme form a square constellation, so the number of symbols can be 4, 16, 64 etc, corresponding to 2, 4, 6, 8 bits per symbol [4].

2.1.1.2 Phase Modulation (PM)

PM is a digital modulation technique in which the phase of the carrier signal is varied in accordance with a digital input signal. In PM, the modulating signal is a digital signal that has a series of discrete values that represent the digital data to be transmitted [4]. The carrier signal used in PM is a sinusoidal waveform with a fixed frequency and amplitude. In PM modulation, the phase of the carrier signal is varied in proportion to the amplitude of the modulating signal. The modulating signal is used to control the phase of the carrier signal, which results in a modulated signal with varying phase. The phase of the carrier signal at any given time represents the digital data being transmitted. There are three types of PM, including Phase Shift Keying (PSK), Differential Phase Shift Keying (DPSK), and Offset Phase Shift Keying (OPSK) [6].

In PSK modulation, the phase of the carrier signal is shifted by a fixed amount for each symbol of the modulating signal. The amount of phase shift corresponds to the digital value being transmitted. For example, in Binary Phase Shift Keying (BPSK), the phase of the carrier signal is shifted by 180 degrees for a binary 1 and remains unchanged for a binary 0. In DPSK, the phase of the carrier signal is varied to represent digital data, but unlike traditional PSK, the phase shift is based on the difference between adjacent symbols rather than the absolute phase. In OPSK, the phase of the carrier signal is varied to represent digital data, but the phase shift is restricted to a limited set of values that are orthogonal to each other [4] [5].

In CPFSK modulation, the phase of the carrier signal is varied in accordance with the frequency of the modulating signal [6].

2.1.2 Large-Scale Fading

An electromagnetic wave propagating through an environment is subjected to reflection, scattering, and diffraction by large-scale objects. A wireless radio channel poses as a severely hostile propagation environment and large-scale objects such as buildings and walls cause long-term impediments to the wave propagating through. These variations occur over large distances, higher than the wavelength, and thus are called large-scale fading [3]. These variations of received power can be simulated using deterministic, empirical or statistical models [4].

2.1.2.1 Path Loss

Path loss represents the amount of power lost due to its dissipation over distance. The general free space path loss equation with no system loss is given by [6]:

$$PL_F(d)[dB] = 10\log\left(\frac{P_t}{P_r}\right) \quad (2.3.)$$

where

d - distance of propagation

P_t - the transmitted power

P_r - the received power given by:

$$P_r(d) = \frac{P_t G_t G_r \lambda^2}{(4\pi)^2 d^2 L} \quad (2.4.)$$

where

More robust empirical path loss models for outdoor environments have been developed since the emergence of wireless transmission technology such as the Hata-Okumura model, Piecewise Linear model, or Nakagami model. In the case of indoor transmission, the type of indoor progpagation environment needs to be accounted for to be added to a chosen empirical path loss model. The indoor propagation factor depends on the layout of the indoor environment, positioning of floors, walls, placement of windows. The number of floors also plays a role in the overall attenuation as attenuation per floor is always highest for the first floor and decreases in higher levels. Materials used for partition segments between the floors are accounted from using the partition attenuation factor. The penetration loss also needs to be included. However, for the purposes of large-scale open area-buildings, a simplified path loss model can be used where the received power is given:

$$P_r = P_t K \left[\frac{d_0}{d}\right]^{\gamma} \quad (2.5.)$$

where $K = 20log_{10}\frac{\lambda}{4\pi d_0}$, d_0 is the reference distance for antenna far-field, and γ is the path loss exponent [6].

2.1.2.2 Shadowing

Shadow fading relates to the signal power fluctuation over large distances and is caused by objects blocking the signal path. Shadowing is usually simulated using statistical models such as the log-normal shadowing model. When combining with the simplified path loss model, a ratio of transmitted and received power in dB is given by:

$$\frac{P_r}{P_t}(dB) = 10log_{10}K - 10\gamma log_{10}\frac{d}{d_0} - \psi_{dB} \quad (2.6.)$$

where ψ_{dB} represents a Gauss random variable [6].

2.1.3 Small-Scale Fading

2.1.3.1 Rayleigh Fading

Small-scale fading refers to rapid fluctuations in amplitude, phase and frequency of the received signal. This is caused by reflection, diffraction and scattering of the signal while encountering small-scale obstacles and irregularities within the propagation medium. Small-scale fading can be represented using the Rayleigh fading statistical model. The Rayleigh Channel model applies when there is not a dominant LOS signal in the channel and there are at least more than three component signal vectors with arbitrary phases and similar amplitude [7]. The probability density function of the Rayleigh channel for signal waveform x can be expressed as:

$$p(x) = \frac{2x}{b^2}\exp\left(-\frac{x^2}{b^2}\right) \quad (2.7.)$$

With the cumulative probability distribution function

$$F(x) = 1 - \exp\left(-\frac{x^2}{b^2}\right) \quad (2.8.)$$

where b is the root mean square value of a Rayleigh component and both x and b are amplitude values [5].

The Rician fading applies when there is a dominant LOS signal present in the channel or in addition there is a strong ground-reflected signal reflected from a rough surface. The probability density function is:

$$p(r) = \frac{2r}{b^2}\exp\left(-\frac{r^2+a^2}{b^2}\right)I_0\left(\frac{ax}{\sigma^2}\right) \quad (2.9.)$$

The cumulative probability distribution function is given by:

$$1 - F(x) = 2\exp(-k^2)\int_{x/b}^{\infty} vexp(-v^2)I_0\left(\frac{2av}{b}\right)dv \quad (2.10.)$$

where

$$I_0(z) = \frac{1}{\pi}\int_0^{\pi}\exp(-zcos\theta)\,d\theta$$

where a and b represents the LOS and Rayleigh component respectively, σ^2 is the standard deviation, v is the antenna terminal voltage, $k = a^2/b^2$, in dB also known as K-factor is a characteristic variable describing a specific distribution based on the channel scenario and the degree of dominance of LOS component [5].

2.1.3.2 Rician Fading

The Rician fading applies when there is a dominant LOS signal present in the channel or in addition there is a strong ground-reflected signal reflected from a rough surface. The probability density function is:

$$p(r) = \frac{2r}{b^2}\exp\left(-\frac{r^2+a^2}{b^2}\right)I_0\left(\frac{ax}{\sigma^2}\right) \quad (2.11.)$$

The cumulative probability distribution function is given by:

$$1 - F(x) = 2\exp\left(-k^2\right)\int_{x/b}^{\infty} vexp(-v^2)I_0\left(\frac{2av}{b}\right)dv \quad (2.12.)$$

where

$$I_0(z) = \frac{1}{\pi}\int_0^{\pi}\exp(-zcos\theta)\,d\theta$$

where a and b represents the LOS and Rayleigh component respectively, σ^2 is the standard deviation, v is the antenna terminal voltage, $k = a^2/b^2$, in dB also known as K-factor is a characteristic variable describing a specific distribution based on the channel scenario and the degree of dominance of LOS component [5].

2.2 Multiple Input Multiple Output System (MIMO)

The utilization of multiple antennas can enhance system performance either by increasing the data rates through multiplexing or by improving the reliability through diversity as well as minimizing the intersymbol interference (ISI). Thanks to having multiple antennas the MIMO-based system can take advantage of the presence of multipath components to increase the data rate and channel capacity. MIMO system extends the traditional simplistic communication system model consisting of a single pair of transmitter and receiver antennas to a system where both the transmitter and the receiver consist of multiple antennas [4]. A MIMO system can be simply represented by:

$$\boldsymbol{y} = \boldsymbol{H}\boldsymbol{x} + \boldsymbol{n} \quad (2.13.)$$

where

$\boldsymbol{H}$ - the channel gains matrix of size $M_t \times M_t$, where M_t is the number of transmitter antennas.

$\boldsymbol{x}$ – transmitted data vector

$\boldsymbol{n}$ – noise vector

In Multi-Input Multi-Output (MIMO) systems, the fading channel between each transmit and receive antenna pair can be modelled as a Single-Input Single-Output (SISO) channel. This is because for small element spacings, the path loss and shadowing of all SISO channels are identical. Therefore, each transmit and receive antenna pair can be treated as a separate SISO

channel with the same channel characteristics, and the MIMO channel can be decomposed into multiple independent SISO channels. This simplifies the analysis and design of MIMO systems, as the techniques developed for SISO channels can be applied to each independent SISO channel [5].

Different hypotheses can be made concerning the understanding of the channel gain matrix H by the transmitter and receiver, denoted as channel side information at the transmitter (CSIT) and channel side information at the receiver (CSIR), respectively. In the case of a stationary channel, it is typically assumed that CSIR is available, as the channel gains can be acquired without much difficulty by transmitting a pilot sequence for channel estimation. In situations where both the transmitter and the receiver have no knowledge of the channel, it is necessary to assume a probability distribution for the channel gain matrix [4]. This can be done for example by using space-time coding schemes. CSI knowledge also lowers the decoding complexity at the receiver for higher order modulation schemes [5] [4].

2.2.1 Diversity

The purpose of diversity is to improve the system's performance by increasing the reliability of the transmission, since the probability of all the signal paths fading simultaneously is lower than the probability of a single path fading. In MIMO systems, diversity is achieved by using a combining scheme that merges a number of independently fading signal paths, where the same signal is transmitted through multiple fading paths [4]. By selecting an efficient combining scheme, the effects of fading can be reduced or eliminated. The combining scheme can be chosen based on the type of fading channel, the number of antennas, and the system requirements. Effective combining schemes can mitigate the effects of fading, resulting in improved system performance. MIMO systems use multiple transmit or receive antennas, arranged in an antenna array, where the elements are separated in distance. This arrangement is known as space diversity. To achieve a unit rank input covariance matrix, the same symbol is transmitted over each transmit antenna, a technique called beamforming. In MIMO-based systems, beamforming is performed at the transmitter end while at the receiver end, equal-gain combining (EQC) technique is applied.

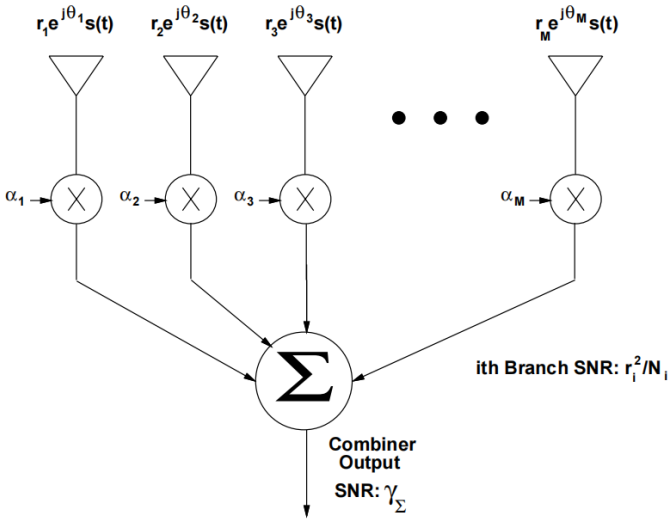

Figure 2.2.: Diversity Combiner [4].

EGC is a type of receiver diversity combining technique that co-phases the signals on each branch and combines them with equal weighting. This technique is used to improve the received signal power and to reduce the effects of fading by selecting the best signal path from multiple independently fading channels. Figure 2.2. shows a diversity combiner schematic. Each receiver receives a different version of signal $s(t)$. Each signal has a different power and phase which is determined by the position of each receiver antenna. In the case of EGC, all weights α_m are equal [5]. The SNR of EQC technique output is given by:

$$\gamma_{\Sigma} = \frac{1}{N_0 M} \left(\sum_{m=1}^{M} r_m\right)^2 \tag{2.14.}$$

where

N_0 – noise power spectral density

M – number of branches

r_m – signal power of the mth branch

2.2.2 Multiplexing

Multiplexing is a technique used in wireless communication systems to increase the capacity of a network by transmitting multiple signals simultaneously over a single channel. Multiplexing in MIMO systems can be achieved through two main techniques: spatial multiplexing and time-division multiplexing. The multiplexing gain is given by [4]:

$$R = \sum_{m=1}^{M_r} \log_2(1 + \rho s_m \sigma_m^2) \tag{2.15.}$$

where

M_r – number of receiver antennas

s_k – power allocation for each channel element

σ_k - channel element for SIS channels of the decomposed MIMO channel by singular value decomposition.

2.2.3 Precoding

2.2.3.1 Zero-forcing (ZF)

Zero-forcing precoding technique is a representative of linear signal detection precoding techniques. The objective of ZF precoding is to invert the channel matrix, allowing the transmitted signal to be aligned with the desired signal at the receiver. This technique cancels out the interference from other signals that are transmitted concurrently, improving the signal quality and system performance. ZF is used in MU-MIMO systems where each user consists of one receiver antenna. The main idea behind ZF beamforming is to force the interference to zero. Assume having a transmitted signal $\boldsymbol{x}$, the transmitted signal vector can be represented as [5]:

$$\boldsymbol{x} = [x_1, x_2, \dots, x_M]^T$$

where x_m is the signal transmitted from the m-th antenna.

The goal of ZF is to find a beamforming weight vector w that minimizes the interference at the receiver by making the interference orthogonal to the receive antenna. The beamforming weight vector can be represented as:

$$\boldsymbol{w} = [w_1, w_2, \dots, w_M]^T$$

he transmitted signal after applying the beamforming weights is:

$$\boldsymbol{s} = \boldsymbol{w}^H \boldsymbol{x}$$

The received signal after applying the beamforming weights can be expressed as:

$$\boldsymbol{y} = \boldsymbol{w}^H \boldsymbol{H}\boldsymbol{x} + \boldsymbol{n}$$

To achieve zero interference, it is required to make sure that the beamforming weights $\boldsymbol{w}$ are chosen such that:

$$\boldsymbol{w}^H \boldsymbol{H}\boldsymbol{h}_m = 0 \text{ for all } m = 1, 2, \dots, M$$

where is the $\boldsymbol{m}$-th column of the channel matrix $\boldsymbol{H}$.

In matrix form, this can be expressed as:

$$\boldsymbol{H}^H \boldsymbol{H}\boldsymbol{w} = 0$$

Solving for $\boldsymbol{w}$ will provide the desired precoding matrix and will be explained in Section 3.

2.2.3.2 Block Diagonalization (BD)

Block-diagonalization precoding (BD) is an extension of the zero forcing (ZF) precoding technique used in multi-user multi-antenna communication systems. BDP overcomes the limitations of ZF, which is known to perform poorly when the number of transmit antennas is greater than the number of users [4].

In BD, the transmitter divides the users into disjoint groups and applies ZF precoding to each group independently. This results in a block-diagonal structure in the equivalent channel matrix, where the diagonal blocks correspond to the individual groups of users. Since the off-diagonal blocks are zeroed out, the interference among the different groups of users is eliminated.

The main advantage of BD is that it can achieve the same performance as ZF for the case where the number of transmit antennas is greater than the number of users. This is because the precoding problem is reduced to several smaller independent problems, each involving a subset of the antennas and a subset of the users.

Mathematically, the channel matrix H can be partitioned into submatrices as follows [5]:

$$\boldsymbol{H} = [\boldsymbol{H_1}, \boldsymbol{H_2}, \ldots, \boldsymbol{H_U}]$$

where $\boldsymbol{H_k}$ is the channel matrix for user u, and U is the total number of users sharing the channel.

The precoding matrix can be designed to have a block diagonal structure, such that it separates the transmit signal into non-interfering subspaces:

$$\boldsymbol{P} = [\boldsymbol{P_1}, \boldsymbol{P_2}, \ldots, \boldsymbol{P}_U]$$

where $\boldsymbol{P}_U$ is the precoding matrix for user U.

The transmitted signal vector s can then be expressed as:

$$\boldsymbol{s} = \boldsymbol{Px}$$

where $\boldsymbol{x}$ is the vector of symbols to be transmitted. The received signal vector $\boldsymbol{y}$ can be expressed as:

$$\boldsymbol{y} = \boldsymbol{Hs} + \boldsymbol{n}$$

where n is the vector of additive noise.

Substituting $\boldsymbol{s} = \boldsymbol{Px}$, we get:

$$\boldsymbol{y} = \boldsymbol{HPx} + \boldsymbol{n}$$

Pre-multiplying by the pseudo-inverse of HP, we get:

$$(\boldsymbol{P^H HP})^{-1}\,\boldsymbol{P^H y} = (\boldsymbol{P^H H})^{-1}\,\boldsymbol{x} + (\boldsymbol{P^H HP})^{-1}\,\boldsymbol{P^H n} \quad (2.16)$$

The first term on the right-hand side of the equation represents the non-interfering subspace for each user, and the second term represents the residual interference caused by other users [4].

2.3 RIS Concept

A reflective intelligent surface (RIS) is made up of densely populated scattering elements, each with dimensions smaller than the wavelength. As the element size decreases, more elements can be fitted into the same area, which increases the accuracy of beamforming by expanding the channel and impedance matrices [1]. The scattering elements are equipped with programmable diodes that modify their impedance pattern based on instructions from the precoding matrix. RIS has the advantage of being passive, requiring minimal input power or potentially using power received from the transmitter [2]. This technology has the potential to revolutionize wireless communication systems by providing an efficient and cost-effective solution for improving signal quality and coverage.

The presence of RIS allows for a significant alteration for the effective channel and thus can be expanded to [1]:

$$\boldsymbol{y} = \boldsymbol{x}(\sqrt{G_d}\boldsymbol{H}_{env} + \sqrt{G_r}\boldsymbol{H}_{RIS}) + \boldsymbol{n} \quad (2.17.)$$

where $\boldsymbol{H}_{env}$ represents the canonical channel based on the propagation distribution model of choice and $\boldsymbol{H}_{RIS}$ represents the contribution of the RIS-assisted channel.

$\boldsymbol{H}_{RIS}$ varies and is dependent on chosen channel model, depending on the RIS implementation.

The channel follows the concept of a diadic backscatter channel model, thus the $\boldsymbol{H}_{RIS}$ model can be represented by

$$\boldsymbol{H}_{RIS} = \boldsymbol{FQC} \quad (2.18.)$$

Where $\boldsymbol{F}$ represents the channel between RIS and the receiver, $\boldsymbol{G}$ represents the channel between the transmitter and RIS, and $\boldsymbol{Q}$ represents the effect of RIS on the transmitted signal waveform, mainly the phase shift:

$$\boldsymbol{Q} = diag(\beta_1 e^{i\theta_1}, \beta_2 e^{i\theta_2}, \dots, \beta_L e^{i\theta_L}) \quad (2.19)$$

where $\boldsymbol{\beta_l} \in [0,1]$ represents amplitude of the signal, $\theta_l \in [0,2\pi)$ represents the phase shift, where l represents an individual RIS element [1].

2.3.1 Types of RIS

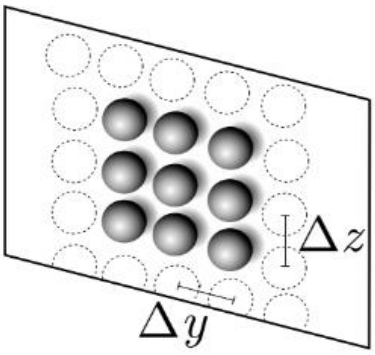

Figure 2.3: Refflectarrya RIS [7]

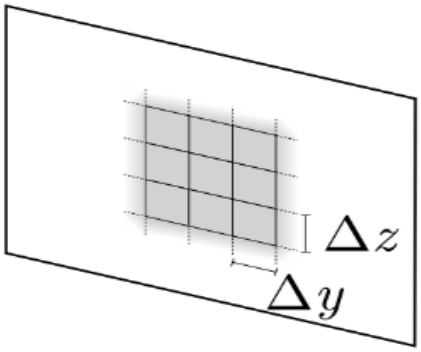

Figure 2.4: Metasurface RIS [7]

There are two ways to implement RIS technology: reflectarrays, which use arrays of isotropic antennas with dimensions comparable to half of the signal wavelength, and metasurface planes, which use small planar antennas with sub-wavelength sizes made up of densely packed meta-atoms. While reflectarrays can improve signal quality, metasurface planes offer even greater performance due to the smaller sizes of individual elements and tighter spacing distances between them. This enables more meta-atoms to be packed into a single scattering element, resulting in a higher number of controllable variables and improved beamforming accuracy. As a result, metasurface planes are considered a more efficient and effective implementation of RIS technology [1] [7] .

2.3.2 Limitations

2.3.2.1 Channel State Information (CSI)

To optimize the phase shift of RIS, channel information is necessary. However, since RIS are primarily passive objects, sending pilot pulses to estimate the channel condition is not feasible. To overcome this issue, feedback loops between the RIS and the receiver have been established with positive results reported using various implementations. Another approach is to dedicate a small subset of RIS elements to estimate the channel by processing pilots sent by both the transmitter and the receiver. While this approach requires a small amount of energy consumption, it provides a more accurate channel estimation and improves the overall

performance of the system. Overall, there are several methods available to address the channel information issue for RIS, each with its own advantages and disadvantages [1].

2.3.2.2 Near-field Characteristics

Near-field effects are another problem that can arise when using RIS in wireless communication systems. The near-field region is the area surrounding the RIS where the electromagnetic fields are complex and vary significantly with distance, resulting in unpredictable signal behavior. In contrast, the far-field region is where the electromagnetic fields have a more uniform and predictable behavior.

The near-field effects can cause significant challenges when deploying RIS, as they can impact the accuracy of beamforming and degrade the overall system performance. One solution to this problem is to use a multi-objective optimization framework that takes into account both the far-field and near-field effects. This can help to optimize the placement of the RIS elements and the control of the phase shifts to achieve the desired performance while minimizing the near-field effects [2].

2.3.2.3 Mutual Coupling

Mutual coupling is a common problem that arises when using RIS in wireless communication systems. It occurs when the closely spaced elements of the RIS interact with each other, resulting in interference that can degrade the signal quality. The main cause of mutual coupling is the electric and magnetic fields radiated by each element that can reach other elements in the same array. This can cause a significant reduction in the performance of RIS.

To overcome mutual coupling, several techniques have been proposed, including using decoupling elements between the RIS elements or adjusting the distance between the elements to minimize the interaction. Another solution is to employ a calibration procedure to estimate the mutual coupling effects and then compensate for them using digital signal processing techniques.

Although these techniques can improve the performance of RIS, they have some limitations, including increased complexity and cost. Therefore, it is essential to carefully consider mutual coupling effects during the design and deployment of RIS in wireless communication systems. By mitigating mutual coupling, RIS can provide improved signal quality and coverage, making them an attractive solution for next-generation wireless communication systems [7] [32].

3 System Specification

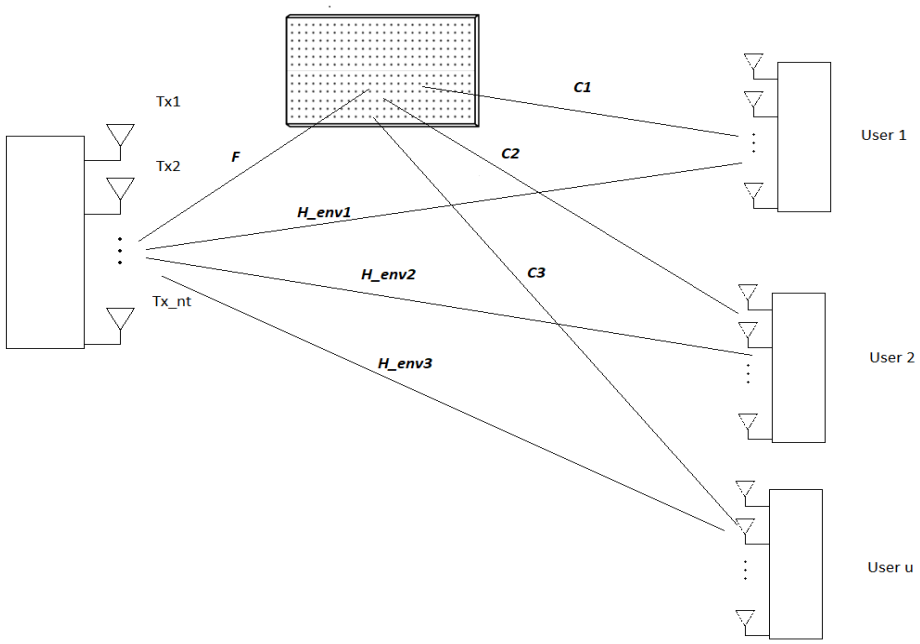

Figure 3.1: RIS-assisted MIMO Communications System

3.1 System Overview

The system designed in this project simulates a full communications link between a base station and 1 and 2 user equipment devices. Both the base station and user devices consist of multiple antennas to simulate the diversity gain through the MIMO system and with a RIS panel placed in between the base station and user equipment. The MIMO sizes tested will be 4x4, 8x8, and 64x64, with the latter being a good basis for looking into massive MIMO applications. The number of RIS elements simulated will vary between 16, 32, and 256. The position of the RIS will be varied between 10 metres and 100 meters from both the base station and one of the user equipment devices to investigate the effect on system performance with the changing displacement between the RIS and antenna arrays. The transmitted signals use the QPSK modulation scheme and are sent through the BS-UE channel and a BS-RIS-UE channel with a combining method being applied at the receiver. The small scale fading model used for this simulation is the Rayleigh fading model and the large scale fading model used is based on the Simplified Path Loss model. The CSI is considered perfect and is known to the transmitter and can thus be used for signal precoding as. The precoding schemes used in this system is the ZF precoding scheme with its extension for a multi-user system, the Block Diagonalization scheme. The signal sent to the RIS is evaluated on arrival at the panel where its arrival angle is

determined and using the information on the correlation between each RIS element the diversity characteristics can be better exploited [7]. The signal received at the receiver end of the system is demodulated and decoded signal is then compared to the transmitted signal from which the BER can be evaluated. This is examined with SNR ranging from 0 to 20 dB.

3.2 Coordinate System

A three-dimensional Cartesian coordinate system is set up to represent the system environment and it is given by the x, y, z axes. The surface is considered to be mounted on a wall vertical to the xy plane in a large indoor venue. The transmitter and receiver antennas are formed by an array of antennas placed in columns vertical to the xy plane. The RIS plane consists of N identical and equally spaced antenna elements. The antenna spacing of both antenna vectors and the RIS array are dependent on the wavelength of the transmitted signal and for the simulated environment are set by default to be half of the wavelength λ, which is the maximal usually considered antenna spacings. The panel can be used for both single-user and multi-user transmission. The positions of the transmitter and receiver antennas and the RIS elements are defined with respect to this coordinate system. The position of each point is given by its coordinates (x,y,z), and distances between elements of each system component are given by pre-determined spacing distances. The coordinates of each component element, be it transmitter and receiver arrays or RIS matrices, are stored in $N \times 3$ matrices [7].

3.2.1 Euclidean Distance

To calculate the path loss using the chosen path loss model equations, a transmitter-RIS and RIS-receiver distances need to be calculated. Given an elements $\boldsymbol{o} = [x_{\boldsymbol{o}}\ y_{\boldsymbol{o}}\ z_{\boldsymbol{o}}]^T$ and $\boldsymbol{p} = [x_{\boldsymbol{p}}\ y_{\boldsymbol{p}}\ z_{\boldsymbol{p}}]^T$, the distance between $\boldsymbol{o}$ and $\boldsymbol{p}$ in the xyz space is given by:

$$d = ||\boldsymbol{o} - \boldsymbol{p}||_2 \qquad (3.1.)$$

3.2.2 Departure Angle and Path loss

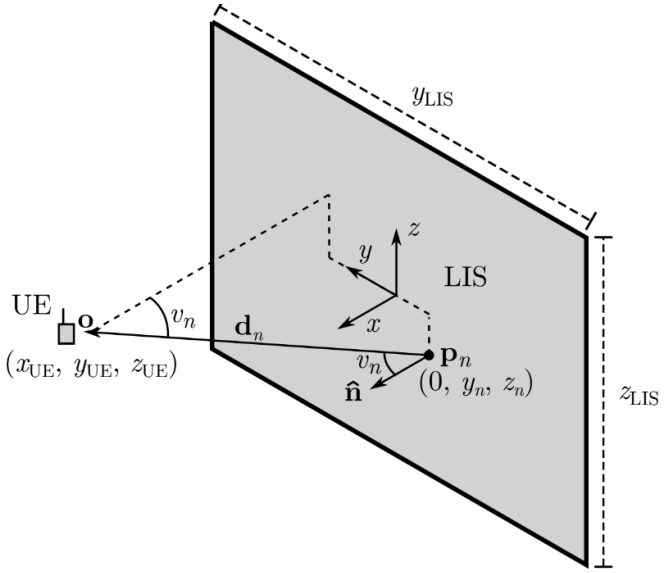

Figure 3.2: Illustration of the Scenario in of Signal Reflected from the RIS towards the Receiver (UE) [7]

Using the Equation .. , this can be derived into an equation for power captured received on the RIS element [31]:

$$P_n^{RIS} = \frac{P_t G_t G_e^{Tx} \lambda^2 \sigma_{RCS}^m}{(4\pi)^2 a_n^2} \tag{3.2.}$$

where

P_t – Transmit Power = 1

G_t –Transmit gain in this project is set to be unity

G_e^{Tx} – RIS gain in the direction of the transmitter

λ – Wavelength

σ_{RCS}^m – Radar cross-section (RCS) of the scattering elements where m is the number of elements

a_n^2 – Distance from the transmitter to the nth interacting object (IO, scatterer) element

The received power at the receiver can be extended to :

$$P_{n_{Rx}}^{Rx} = \frac{P_t G_t G_r G_e^{Tx} G_e^{Rx} \lambda^4 \sigma_{RCS}^m}{(4\pi)^5 a_n^2 b_{m,n}^2 c_n^2} \tag{3.3}$$

where

G_r – Receiver Gain set to be unity

G_e^{Rx} – RIS gain in the direction of the receiver

$b_{m,n}$ – Distance between the mth IO element and nth RIS element

c_n – Distance between the nth RIS element and the receiver

Rearranging Equation, the path loss equation can be derived:

$$L_n = \frac{G_e^{Tx}\lambda^2}{(4\pi)^2 a_n^2} \times \frac{G_e^{Rx}\lambda^2}{(4\pi)^2 b_n^2} \times \frac{1}{4\pi c_n^2} \quad (3.3.)$$

G_e^{Tx} and G_e^{Rx} are the gain of the RIS element in the direction of the transmitter and the receiver respectively and are related the incident angles of the signals arriving at RIS and the departure angles of the signal to the receiver. The gain can be found using [31] [41]:

$$G_e(\psi) = \gamma cos^{2q}(\psi) \quad (3.4.)$$

where

ψ – Incident or departure angle measured from the broadside of the RIS element

γ – power conservation coefficient, can be calculated using:

$$\gamma = 2(2q + 1) \quad (3.5.)$$

to satisfy the power constraint. Factor q determines the gain of each RIS element. While mathematically, each element should have its q factor determined separately, that could be computationally and theoretically challenging and could be a topic for a different paper to discus, for general studies it can be assumed that all elements have the effective aperture area A_e of the identical size of $\left(\frac{\lambda}{2}\right)^2$. The total area of the RIS is thus the sum of all $A_e * N$ when the element spacing is λ/2. This yields a $q = \sim 0.285$ and a $\gamma = pi$.

The incident and departure angles of the signals can be found using [7]:

$$v_a = arccos(\frac{x_b}{d_a}) \quad (3.6.)$$

where

v_a – Desired angle form the broadside of point b towards the direction of point a

x_b – x coordinate of point b

d_a – distance form point a to point b

Note that this path loss model is considered to be used in an open indoor environment only, in case of an outdoor use, some other deterministic path loss model shall be used such as Umi Street Canyon Model [4].

3.3 Impedance Patterns and Correlation

In RIS systems, correlation analysis is an essential tool for optimizing the performance of the surface by adjusting the phase and amplitude of the individual elements.

Correlation analysis in RIS involves computing the correlation coefficient between the signals received at different antennas or elements of the surface. This can be done using various techniques, such as cross-correlation, auto-correlation, and correlation matrix analysis. The results of the analysis can be used to adjust the phase and amplitude of the elements to maximize the coherence of the received signals [7].

RIS systems rely on the principles of signal processing and optimization to enhance the performance of wireless communication systems. By controlling the signals reflected by the surface, RIS can improve the signal-to-noise ratio, increase the coverage area, and reduce the interference between different wireless devices.

While the general Rayleigh fading channel is given by Equation 10, in order to fully exploit the diversity gain of the system, the channel model can be modified to consider the spatial correlation of RIS elements. The modified channel model for one element is thus [44]:

$$\boldsymbol{H_n} = \sqrt{L_p}Zz_k \tag{3.7.}$$

where

L_p – Path loss

Z – correlation matrix

z_k – i.i.d. distributed fast fading element $\sim\ CN\ (0, I_N)$, where I_N is excitation current for an element.

This can be simplified by simply generating the correlation matrix derived in Section .. , which can be rearranged into:

$$z(\boldsymbol{p}_n, \boldsymbol{p}_m) = \left(\frac{sin\left(k||\boldsymbol{p}_n - \boldsymbol{p}_m||_2\right)}{k||\boldsymbol{p}_n - \boldsymbol{p}_m||_2}\right) \tag{3.8.}$$

where

k – wavenumber given by $k = \frac{2pi}{lambda}$

$\boldsymbol{p}_n$ – position of the nth element

$\boldsymbol{p}_m$ – position of the mth element

3.4 Precoding

3.4.1 Zero-forcing

The MIMO ZF receiver has similar features to ZF equalizers in frequency selectie channels described in Section. As ZF filters spred the channel into a number of sub-channels, the

interference from adjacent transmitted symbols is suppressed. Suppose a symbol vector $X = 1/\sqrt{n}[c_1 \dots c_n]^T$ is transmitted, if the ZF precoding is applied, the output will have a form of:

$$\boldsymbol{z} = X + \boldsymbol{G}_{ZF}\boldsymbol{n} \tag{3.9}$$

where

$$\boldsymbol{G}_{ZF} = \sqrt{\frac{n}{E_s}} \times \boldsymbol{W} \tag{3.10.}$$

where

E_s – symbol energy

$\boldsymbol{W}$ the precoding weight matrix. The weight matrix to extinguish ISI in the system can be obtained using the following scheme [11]:

$$\boldsymbol{W} = (\boldsymbol{H}^H\boldsymbol{H})^{-1}\boldsymbol{H}^H \tag{3.11.}$$

It should be noted that the channel model at this time will need to be adjusted due to the presence of RIS and will be in a format of $\boldsymbol{y} = \boldsymbol{H}(\boldsymbol{e}^{j\theta})\boldsymbol{x} + \boldsymbol{n}$

Where $\boldsymbol{e}^{j\theta}$ represents phase change due to RIS.

3.4.2 Block Diagonalization

Block diagonalization should be extended for the purpose of the multi-user RIS scenario, assuming each receiver consists of more than one antenna. For $N_{M,u}$, that is te number of antennas for u users, the system model will now have the following form [5].

$$\begin{bmatrix} \boldsymbol{y}_1 \\ \boldsymbol{y}_2 \\ \vdots \\ \boldsymbol{y}_u \end{bmatrix} = \begin{bmatrix} \boldsymbol{H}_1 & \boldsymbol{H}_1 & \cdots & \boldsymbol{H}_1 \\ \boldsymbol{H}_2 & \boldsymbol{H}_2 & \cdots & \boldsymbol{H}_2 \\ \vdots & \vdots & \ddots & \vdots \\ \boldsymbol{H}_u & \boldsymbol{H}_u & \cdots & \boldsymbol{H}_u \end{bmatrix} \begin{bmatrix} \boldsymbol{W}_1\tilde{\boldsymbol{x}}_1 \\ \boldsymbol{W}_2\tilde{\boldsymbol{x}}_2 \\ \vdots \\ \boldsymbol{W}_u\tilde{\boldsymbol{x}}_u \end{bmatrix} + \begin{bmatrix} \boldsymbol{n}_1 \\ \boldsymbol{n}_2 \\ \vdots \\ \boldsymbol{n}_4 \end{bmatrix}$$

Where $\tilde{\boldsymbol{x}}_U$ represents the set of symbols sent at one instance.

As discussed in Section 2.2. the precoder matrix $\boldsymbol{W}$ must null the channel matrix $\boldsymbol{H}$ **,** thus:

$$\begin{bmatrix} \boldsymbol{y}_1 \\ \boldsymbol{y}_2 \\ \vdots \\ \boldsymbol{y}_u \end{bmatrix} = \begin{bmatrix} \boldsymbol{H}_1\boldsymbol{W}_1 & \boldsymbol{0} & \cdots & \boldsymbol{0} \\ \boldsymbol{0} & \boldsymbol{H}_2\boldsymbol{W}_2 & \cdots & \boldsymbol{0} \\ \vdots & \vdots & \ddots & \vdots \\ \boldsymbol{0} & \boldsymbol{0} & \cdots & \boldsymbol{H}_u\boldsymbol{W}_u \end{bmatrix} \begin{bmatrix} \tilde{\boldsymbol{x}}_1 \\ \tilde{\boldsymbol{x}}_2 \\ \vdots \\ \tilde{\boldsymbol{x}}_u \end{bmatrix} + \begin{bmatrix} \boldsymbol{n}_1 \\ \boldsymbol{n}_2 \\ \vdots \\ \boldsymbol{n}_4 \end{bmatrix}$$

To find the weights that satisfy such a relationship, a singular value decomposition of the $\boldsymbol{H}_u$ needs to be performed, thus giving:

$$\widetilde{\boldsymbol{H}_u} = \widetilde{\boldsymbol{U}_u}\,\widetilde{\Lambda_u}\,[\widetilde{V_u}^{non-zero}\,\widetilde{V_u}^{zero}]^H \tag{3.12.}$$

where

$\widetilde{\boldsymbol{H}_u}$ - sub-matrix of the overall channel matrix $\boldsymbol{H}$ corresponding to user u

$\widetilde{\boldsymbol{U_u}}$ - unitary matrix $\boldsymbol{U}$ corresponding to the SVD of the sub-matrix $\widetilde{\boldsymbol{H_u}}$

$\widetilde{\Lambda_u}$ - diagonal matrix of singular values corresponding to the SVD of the sub-matrix $\widetilde{\boldsymbol{H_u}}$

$\widetilde{\boldsymbol{V}_u}^{non-zero}$ – matrix composed by singular vectors corresponding to the SVD of the sub-matrix $\widetilde{\boldsymbol{H_u}}$, but with only the columns corresponding to non-zero singular values

$\widetilde{\boldsymbol{V}_u}^{zero}$ - matrix composed by singular vectors corresponding to the SVD of the sub-matrix $\widetilde{\boldsymbol{H_u}}$, but with only the columns corresponding to zero singular values

When multiplying $\boldsymbol{H}_u$ and $\widetilde{\boldsymbol{V}_u}^{zero}$, the following relationship applies:

$$\boldsymbol{H}_u\boldsymbol{V}_u = \widetilde{\boldsymbol{U}_u}[\widetilde{\Lambda_u}\ \ \boldsymbol{0}]\begin{bmatrix}\left(\widetilde{\boldsymbol{V}_u}^{non-zero}\right)^{\boldsymbol{H}} \\ \left(\widetilde{\boldsymbol{V}_u}^{zero}\right)^{\boldsymbol{H}}\end{bmatrix}\widetilde{\boldsymbol{V}_u}^{zero}$$

$$= \widetilde{\boldsymbol{U}_u}\,\widetilde{\Lambda_u}^{non-zero}\left(\widetilde{\boldsymbol{V}_u}^{non-zero}\right)^{H}\widetilde{\boldsymbol{V}_u}^{zero}$$

$$= \widetilde{\boldsymbol{U}_u}\,\widetilde{\Lambda_u}^{non-zero}\,\boldsymbol{0} = \boldsymbol{0}$$

This means that if there is a transmission from the transmitter towards the direction $\boldsymbol{V}_u$, only the uth ser receives the signal, thus $\boldsymbol{W}_u = \widetilde{\boldsymbol{V}_u}$ [5].

3.5 Channel Model

After the transmitter and receiver parameters and positions have been determined, and all the calculations for angular and displacement parameters have been performed, a spatial channel model can be eventually designed. Each signal will be transmitted with an input power P_{in} of a value of unity. The angles of arrival of the signal at the RIS element will be calculated using Equation … The transmit signal will be precoded using the ZFBD precoding scheme and the signal will be reflected to the position of the destination at angle which can be calculated by Equation ..

The overall channel model model

$$H_{RIS} = h_{RIS}(n_r, n_t) = \sqrt{\frac{1}{2}}\left(x_{n_t,n_{RIS}} + jy_{n_t,n_{RIS}}\right)\sqrt{d_{n_T,n_{RIS}}^{-\alpha}}$$

$$\times\, diag\left(\frac{q_{n_{RIS}}^{Rand}\sin\left(k\left\|\boldsymbol{p}_{n_{RIS}}-\boldsymbol{p}_{n_{RIS+1}}\right\|_2\right)}{k\left\|\boldsymbol{p}_{n_{RIS}}-\boldsymbol{p}_{n_{RIS+1}}\right\|_2}\right)\times\sqrt{\frac{1}{2}}\left(x_{n_{RIS},n_r}+jy_{n_{RIS},n_r}\right)\sqrt{d_{n_{RIS},n_r}^{-\alpha}} \quad (3.13.)$$

where

$x_{n_t,n_{RIS}}$ – real i.i.d. random variable of the n_tth transmitter to n_{ris}th RIS element channel following a standard normal (Gaussian) distribution with mean 0 and variance 1

$y_{n_t,n_{RIS}}$ – imaginary i.i.d. random variable of the n_tth transmitter to n_{ris}th RIS element channel following a standard normal (Gaussian) distribution with mean 0 and variance 1

x_{n_{RIS},n_r} – real i.i.d. random variable of the n_{RIS}th transmitter to n_rth RIS element channel following a standard normal (Gaussian) distribution with mean 0 and variance 1

y_{n_{RIS},n_r} - imaginary i.i.d. random variable of the n_{RIS}th transmitter to n_rth RIS element channel following a standard normal (Gaussian) distribution with mean 0 and variance 1

$d_{n_T,n_{RIS}}^{-\alpha}$ - path loss factor between the n_Tth transmitting antenna and the n_{RIS}th reflecting element on the RIS panel

$d_{n_{RIS},n_r}^{-\alpha}$ - path loss factor between the n_{RIS}th reflecting element and the n_rth receiving antenna

$q_{n_{RIS}}^{Rand}$ – n_{ris}th phase shift element of the randomized phase shift matrix

k - wavenumber given by $k = \frac{2pi}{lambda}$

$\boldsymbol{p}_{n_{RIS}}$ – position of the n_RISth element position

System Parameter	Description
Modulation Order	4 (QPSK)
MIMO Array Size	4x4, 8x8
Input Power	1 W
Number of Reflecting Elements in the RIS	16, 64
~Distance of RIS from the Receiver	10 m
Carrier Frequency	2.49 GHz
Number of Users with Multiantenna receivers	1, 2
Precoding Schemes Applied	Zero-forcing, Block Diagonalization
Fading Model	Rayleigh
Path Loss Model	Friis Model, later with scatterer deployment
Antenna Gain	1

Table 1: System Parameters

4 Implementation

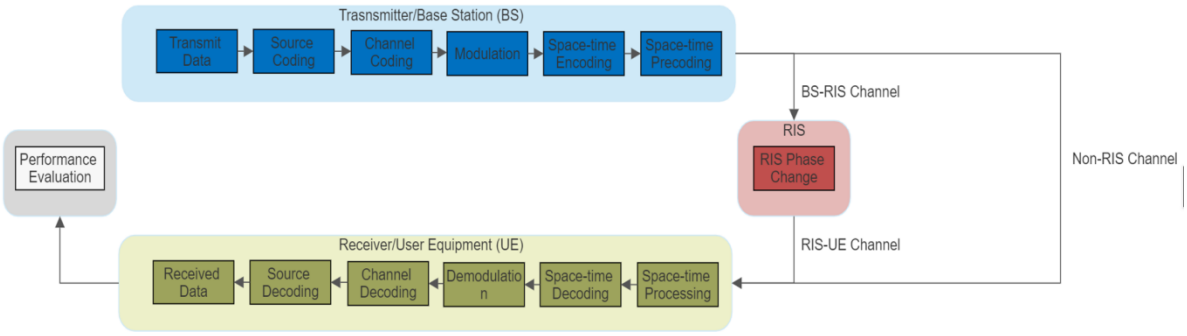

Figure 4.1: System Diagram

System diagram is shown in Figure 4.1. The transmitted signal is encoded, modulated, and precoded. The precoding schemes used for the simulation are the zero-forcing precoding and its extension for multi-antenna multi-user scenarios, the block diagonalization precoding scheme. The signal is sent through two channels, the direct transmitter to receiver channel follows the Rayleigh channel model. The second channel consists of two sub-channels, the transmitter to RIS channel F and the RIS to receiver channel C. The signal is beamformed at the RIS using the phase shift matrix which is a randomized matrix multiplied by the correlation matrix which is obtained by determining the correlation between the RIS elements. At the receiver end, the received signal is decoded using the equal gain combining technique and demodulated to obtained the data message. The message is compared to the original transmitted data to obtain the bit-error rate. The path loss is also calculated for the system and follows the Friis path loss model for free space. However, a more representative path loss model adjusted by the presence of randomly generated scatterers was proposed in Section 3.2.2 as well.

4.1 Element Positioning

The carrier frequency was chosen, from which the wavelength could be obtained. Antenna and RIS element spacing is chosen and is expressed as a ratio of the signal wavelength λ. The position of the first element is chosen at the beginning and using a *for* loop, the *z* coordinate is incremented by spacing distance $d = \frac{1}{2} \times \lambda$ for N_t and N_r iterations respectively where N_t and N_r are the number of transmitter and receiver antennas per user, the positions of each element is stored within a column vector. For the RIS panel, the matrix size is determined where each matrix element represent a RIS element in reality. The elements are displaced with an element

spacing distance $d_{RIS} < \frac{1}{2} \times \lambda$. The number of iterations is equal to the total number of RIS elements.

4.2 Distance and Angle Calculations

Distances between each transmitter element an RIS element are calculated using Equation for N_t iterations. A MATLAB function *norm* can be used, and the distance matrix is of size $N_{RIS} \times N_t$.

For distances between the RIS panel and the given number of user devices (receivers), the same Equation is used, however, N_{USERS} matrices will be generated where N_{USERS} is the number of users, each matrix will be of size $N_{RIS} \times N_r$.

In order to obtain the correlation matrix, the distances between a chosen reference point and each RIS element will need to be found as well using the Equation. Using Equation, the correlation matrix can be obtained using the obtained element distances.

4.3 Signal Data Generation

At the beginning, the number of transmitted symbols is chosen. This number should be chosen while leveraging the result accuracy and computational complexity factors. The number of symbols also indicates the number of iterations of simulations during which each symbol will be transmitted through the designed channel model. The transmitted data is generated using the MATLAB *randi* function. The *randi* function is a MATLAB built-in function that generates a random array of integers. The function syntax for the simulation implementation is given as *randi([0 M-1], N_r, 1),* which means that one symbol is generated per iteration, and the symbol is an integer chosen within a range from 0 to M-1, where M is the modulation order.

4.4 Modulation

The modulation scheme used in this code is PSK (Phase Shift Keying). PSK is a digital modulation technique where the phase of the carrier signal is changed to represent different symbols. In this code, the symbols are integers between 0 and m-1, where m is the modulation order. The modulation order m is a parameter that can be set to different values depending on the desired data rate and system complexity. For example, if m=4, the symbols can be represented as 00, 01, 10, and 11, each with a different phase shift of the carrier signal. The modulated signal is then passed through the RIS and transmitted to the receiver. At the receiver, the received signal is demodulated using the same PSK scheme to recover the original symbols.

4.5 Path Loss

In this code, the path loss is calculated using the following formula:

$$P_n^{RIS} = \frac{P_t G_t G_e^{Tx} \lambda^2}{(4\pi)^2 a_n^2} \quad (4.1.)$$

The formula calculates the power loss due to the spreading of the electromagnetic waves over distance. Specifically, the path loss is inversely proportional to the square of the distance between the transmitter, the RIS, and the receiver. The term $\left(\frac{\lambda}{4}\right)^2$ represents the cross-sectional area of the antenna aperture, and 4π represents the radiation intensity of the isotropic radiator. By multiplying these two terms with the distance factor, we obtain the path loss value.

The path loss calculation assumes that the signal propagates through free space, without any obstacles or attenuation effects. This is a simplified model that can be refined by taking into account the presence of obstacles and the effect of the environment on the signal propagation.

4.6 Channel Model Implementation

The channel consists totally of two paths, the BS-UE path and BS-RIS-UE path. The BS-UE path consists of NtxNr channel elements and represents a conventional MIMO system.

4.6.1 Correlation

In this code, the correlation between the RIS elements is implemented by calculating the correlation matrix $\boldsymbol{Z}$. The impedance of each RIS element is calculated using the following equation:

The correlation matrix Z is then constructed by reshaping the impedance vector into a grid that represents the RIS elements layout. The matrix represents the correlation between the RIS elements, as it captures the effect of the phase shift and reflection of the incident signal at each RIS element. The matrix is used in the beamforming calculation to optimize the signal transmission through the RIS. Specifically, the ZF weight vector is calculated using $\boldsymbol{Z}$ to minimize the interference caused by the correlation between the RIS elements.

4.6.2 Precoding

4.6.2.1 Zero-forcing

The precoding technique implemented in this code is used to optimize the signal transmission through the RIS and mitigate the interference caused by the correlation between the RIS elements. To implement the ZF technique, the channel matrix is first calculated using Equation. Next, the ZF weight vector $\boldsymbol{W}$ is obtained by multiplying the pseudo-inverse of the product of H and its conjugate transpose with the transmitted signal vector. The ZF weight vector is designed to cancel out the interference caused by the correlation between the RIS elements and to maximize the signal power at the receiver end. The transmitted signal is then

multiplied by the ZF weight vector to obtain the beamformed signal, which is transmitted through the RIS and received at the receiver end. Additive white Gaussian noise (AWGN) is added to the received signal to model the effect of noise in the communication channel. Finally, the received signal $\boldsymbol{y}$ is demodulated using the same PSK modulation scheme used in the modulation step to recover the original symbols.

4.6.2.2 Block Diagonalization

The channel matrix (H) is calculated for each user between their receiver antennas and RIS elements.

The SVD (Singular Value Decomposition) of the channel matrix is performed for each user, resulting in the matrices U, S, and V.

The block diagonalizing matrix W is calculated by selecting the columns of V corresponding to the strongest singular values (in this case, the third and fourth columns).

The equalizer matrix (EQ) is calculated as the pseudo-inverse of the product of the block diagonalizing matrix and the channel matrix after applying the block diagonalizing matrix.

This procedure ensures that the interference between different transmitter and receiver antenna pairs is minimized, and the signal-to-interference-plus-noise ratio (SINR) at each receiver antenna is maximized. By using the equalizer matrix, the received signals can be optimally combined to improve the quality of the received data.

Note that the block diagonalization technique assumes that the channel is quasi-static, meaning that it does not change significantly during the transmission of a block of symbols.

4.7 Performance Evaluation Criteria

The RIS-assisted channel is expected to have positive effects on the channel performance in terms of SNR. Improving SNR while maintaining low power required for transmission is the main objective of RIS when applied in single-user mode as mentioned in Section 2.2. and thus, will be one of the main criteria for performance evaluation. Efficiency of the precoding scheme can be assessed by another important performance parameter, the BER, while stability of the channel is assessed by outage probability. Data rate is used as a parameter to assess improvements in channel capacity.

4.7.1 Signal to Noise Ratio (SNR)

Signal to noise ratio compares the signal power to the background noise, expressed in dB. SNR is directly related to channel capacity, higher the SNR is, higher the channel capacity is.

4.7.2 Bit Error Rate (BER)

Bit error rate is a percentage of received bits that have been altered due external factors such as noise, interference, fading etc. It is calculated by dividing the number of erroneous bits by the total number of bits.

4.7.3 Outage Probability

Outage probability is the probability of the receiver power being lower than a pre-determined threshold, the probability of service outage within a certain time frame.

4.7.4 Data Rate

Data rate is the amount of data transmitted during a certain time period, with units of bits per second (bps). It is related to channel capacity, which is the maximum data rate a channel can transmit [8]. The maximum achievable data rate (capacity) can be found using:

$$C = B \times \log_2(1 + SNR) \qquad (4.2.)$$

where

B – Signal bandwidth

SNR – received signal-to-noise ratio

5 Results

A sequence of tests and assessments were created to examine how specific parameters influence the signal propagation's effectiveness. The parameters examined are MIMO array sizes, sizes of the RIS panel, and positioning of the RIS panel. Both single user and multiuser scenarios were examined with 1 and 2 users systems considered.

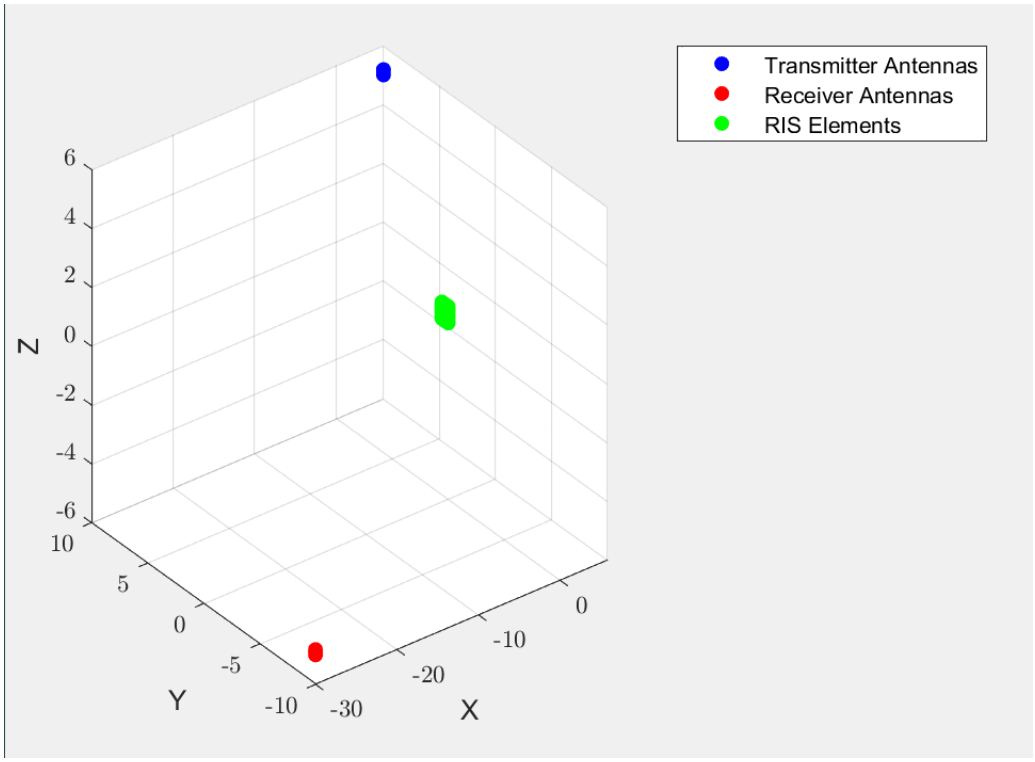

Figure 5.1: Example Scenario Model

5.1 Single-User Scenario

A RIS-assisted system was designed, consisting of a 4x4 MIMO system with an RIS panel placed in between at the distance of 10 m from the base station. The RIS consists of 16 elements. The receiver is considered to represent a single-user device with 4 receiver antennas. The precoding scheme used is the zero-forcing scheme. The system performance in terms of BER is compared to some conventional systems, the SISO direct system following a Rayleigh fading model, the 2x2 MIMO system using the Alamouti space-time block coding and the conventional 4x4 MIMO system with ZF precoding. Results are shown in the Figure 5.2:

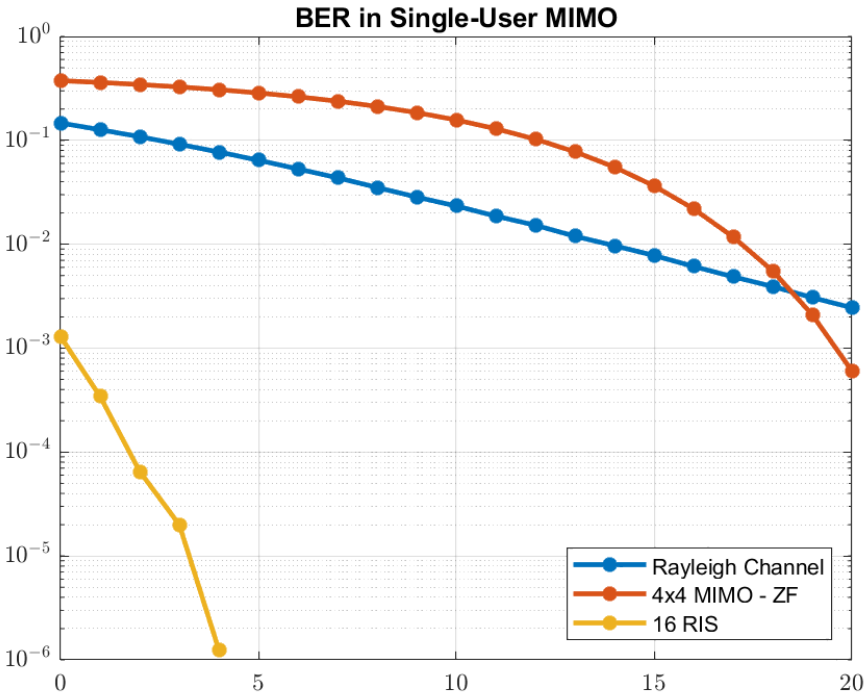

Figure 5.2: BER in Single-User System

It can be observed from Figure 5.2 that the RIS-assisted channel provides an improvement over the conventional MIMO system. The improvement is significant, to achieve the BER of 10^{-4}, the conventional MIMO 4x4 channel requires an SNR of around 25 dB, while with the RIS panel consisting of 16 elements, the SNR required is less than 5 dB. It is observed however, that increasing the number of MIMO array size worsens the performance of the system as can be seen in Figure 5.3. To achieve a BER of 10^{-6}, the conventional 4x4 MIMO system requires SNR of around 25 dB, while the RIS-assisted model requires a SNR of 4 dB only.

System	SNR for BER =10^{-6}
4x4 MIMO – ZF precoding	25 dB
16-element RIS assisted 4x4 MIMO	4 dB

Table 5.1: RIS comparison

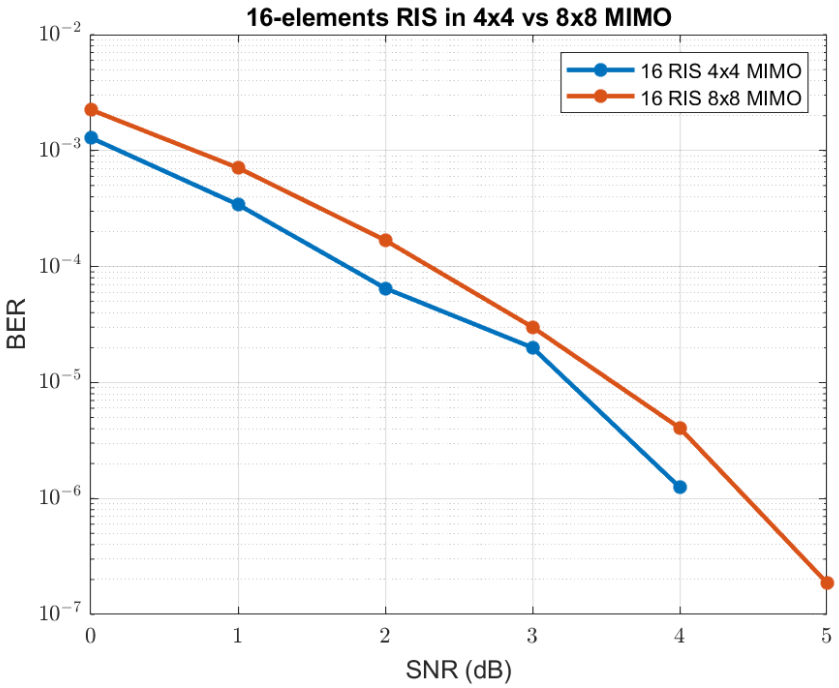

Figure 5.3: 16-element RIS in 4x4 vs. 8x8 MIMO

This can appear as counterintuitive; however, the issue here is with the precoding scheme applied, the ZF precoding. This is due to the fact that ZF precoding completely cancels out the effects of the channel, which can lead to noise amplification and interference from other users. When the number of antennas increases, the channel matrix becomes more ill-conditioned, which means that the inverse of the channel matrix becomes more sensitive to noise and errors. As a result, the performance of ZF precoding can deteriorate as the number of antennas increases [45].

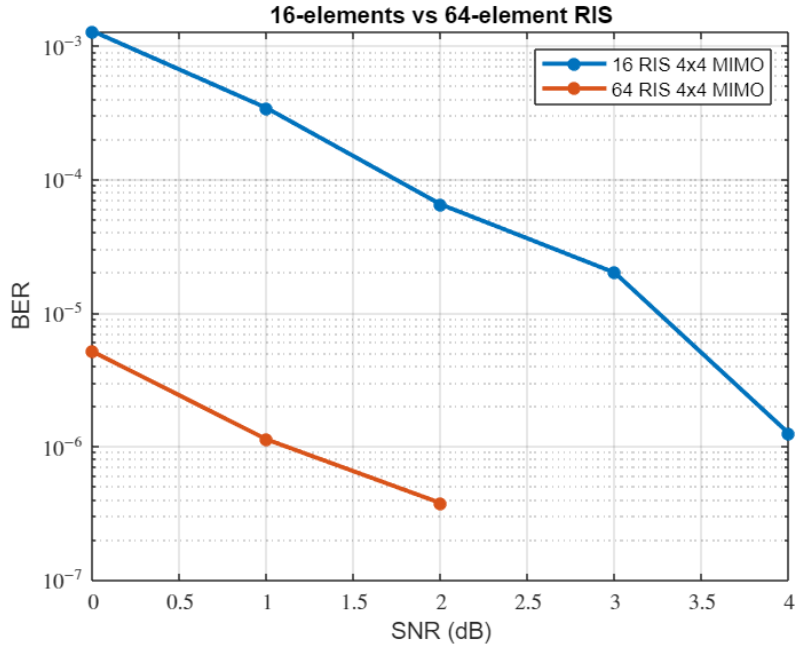

Figure 5.4: 16-elements vs 64-elements RIS

As more scattering elements are placed onto the RIS panel, the system takes advantage of the increased diversity exploit resulting in increased array and multiplexing gain. This can be seen in Figure 5.4 which shows that the 16-element RIS-assisted model required SNR of 4 dB, with 64 elements this was improved to only 1 dB.

System	SNR for BER $=10^{-6}$
16-element RIS assisted 4x4 MIMO	4 dB
64-element RIS assisted 4x4 MIMO	1 dB

Table 3: Impact of the Number of RIS elements

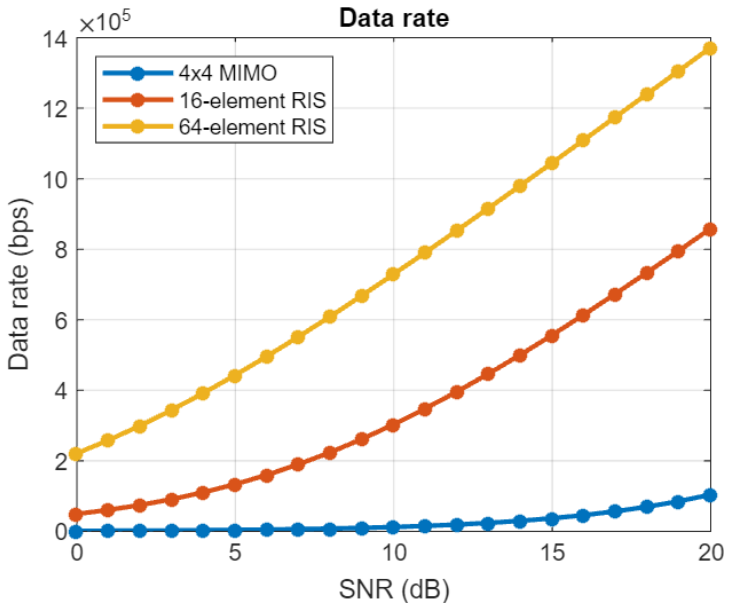

Figure 5.5: Data Rate Comparison

For these reasons, it can also be observed that implementation of RIS within a communication system contributes to significant increases in data rate. A conventional 4x4 MIMO system in a given scenario has a capacity of approximately 100 Mbps at SNR of 20 dB compared to 800 Mbps for a 16-element RIS-assisted system and over 1 Gbps for a 64-element RIS-assisted system as shown in Figure 5.5.

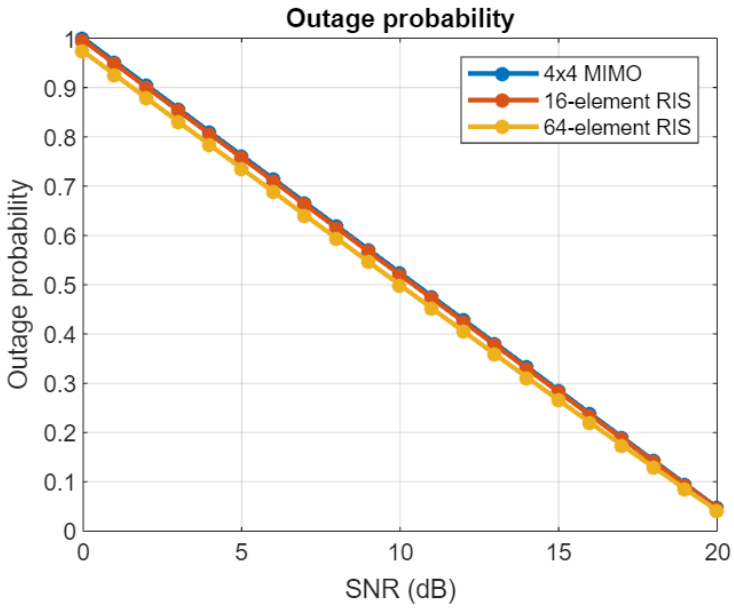

Figure 5.6: Outage Probability

However, in terms of outage probability, there is not a significant improvement observed. On the contrary, the conventional MIMO system shows a negligible, but still observable better performance than the RIS-assisted systems. This could be attributed to the increased interference due to a higher number of transmission-capable elements. The scenario given also considers free space with very few obstructions which are in addition non-large scale. Different scenario of deployment shall be used to better explore the improved stability of RIS-assisted systems.

5.2 Multi-User Scenario

A multi-user RIS-assisted system was designed, consisting of a 4x4 MIMO system with an RIS panel placed in between at the distance of 10 m from the base station. The RIS consists of 16 elements. The receiver is considered to represent a single-user device with 4 receiver antennas. The precoding scheme used is the block diagonalization scheme. The system performance in terms of BER is compared to the non-RIS-assisted 4x4 MIMO system. There are two users, each of them consists of two receiver antennas.

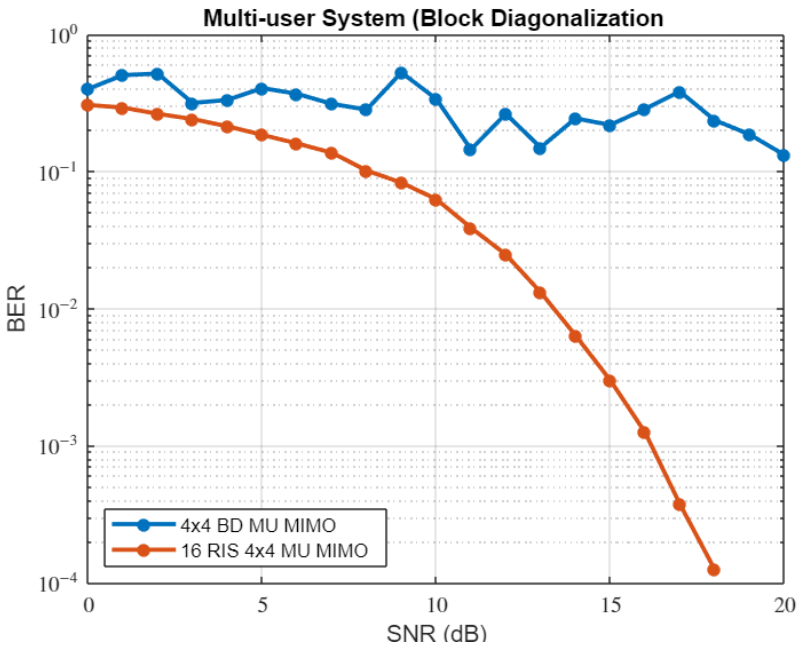

Figure 5.7: Multi-User Scenario

Figure 5.7 shows that RIS deployment in the multi-user MIMO system again significantly increases the performance of the system, however, the performance overall is not as optimized as for the single-user scenario. This can be attributed to interference between the user devices and the previously discussed weakness of the ZF precoding, from which the block diagonalization scheme is derived.

5.2.1.14.3. Overall Results

Overall, the results show that RIS deployment in MIMO systems can provide significant improvement in terms of BER, especially in single-user scenarios. As the number of RIS elements increases exponentially, the 3 dB improvement can be seen for +1 increase of the exponent. The number of scattering elements in the RIS panel and the precoding scheme used play a crucial role in the system's performance. Increasing the number of scattering elements in the RIS panel can improve the system's performance, while the choice of precoding scheme should be carefully considered depending on the specific system requirements and conditions. In multi-user scenarios, interference between the users can also affect the overall system performance, highlighting the need for careful system design and optimization.

6 Project Management

6.1 Project Plan

Within the timeframe specified in the revised Gantt chart included in Appendix A, the project plan was followed through. The novelty of RIS technology required a significant investment of time in reading research papers. As a result of this challenge, the simulation code had to be repeatedly revised as new and improved methods were discovered.

During the first revision, the channel model was modified from a Rayleigh channel model to a spatial channel model for the RIS system application. The Rayleigh channel model proved unsuitable for this project due to its inability to effectively account for reflections. The spatial channel model, on the other hand, automatically considers multiple-input multiple-output (MIMO) properties of the channel, which can be quickly adapted for MIMO simulation if needed, and therefore has several advantages over the Rayleigh channel model and RIS deployment.

During the second revision, the MRT beamforming was revised and changed to the ZF precoding scheme as MRT proved to be rather inefficient and the diversity gain and increase in performance when deploying RIS were not as well observable as for the ZF precoding.

During the third revision, the channel model was revised to account for correlation properties of the signals arriving at the RIS elements. This improved the performance of the system rather than the signals being beamformed by a randomized channel matrix.

The project plan underwent significant changes from the initial Gantt chart in Appendix B to the revised Gantt chart in Appendix A, largely due to numerous revisions in the underlying theoretical foundations. The initial Gantt Chart scheduled making an uplink feedback path for the system to simulate scenarios with imperfect CSI. However, due to the theoretical foundations needed to be applied for the downlink model to develop the project into a more valuable work, and also due to vast amount of theoretical knowledge needed to be acquired to successfully and meaningfully implement the CSI feedback loop, the CSI in the final version of the system is considered perfect. On the other hand, the downlink path was made much more sophisticated than initial objectives required, and the multi-user system was also designed and simulated.

6.2 Budget and Communication

The project primarily involved the use of MATLAB software and did not require any hardware purchases. Progress updates were communicated with Dr Huiling Zhu on a weekly basis to ensure the project was on track.

6.3 Risk Assessment

The software-based nature of this project results in minimal risks, as detailed in Appendix C. The majority of identified risks relate to computer-related fatigue and stress, which can be mitigated by taking frequent breaks away from the computer.

7 Conclusions and Future Work

7.1 Conclusions

This dissertation reports the project undertaken on the topic of deployment of RIS. The project evaluated the performance of a communication link with an assistance of RIS in the system in various scenarios.

7.2 Future Work

7.2.1 Channel -State Information (CSI)

With respect to RIS, there are several methods available for CSI acquisition, each with its own advantages and disadvantages. One approach is to use dedicated pilot elements on the RIS panel to estimate the channel between the RIS and the receiver. The pilot signals can be sent by the transmitter and reflected by the RIS to the receiver. The receiver then uses the received pilot signals to estimate the channel characteristics and provide feedback to the transmitter for signal optimization.

Another approach for CSI acquisition with RIS is to use the feedback loop between the RIS and the receiver. In this approach, the RIS adjusts the phase shift of its elements based on the feedback received from the receiver, which helps to optimize the signal transmission parameters and improve the overall system performance.

In addition, machine learning-based techniques can also be used for CSI acquisition with RIS. These methods can use the data collected from the RIS and the receiver to train machine learning algorithms that can estimate the channel characteristics in real-time.

7.2.2 Moving Receiver

In a radio communication system that employs a Reflecting Surface (RIS), the location of the receiver is critical to achieving optimal performance. The RIS acts as a reflector that reflects the signal towards the receiver, and the position of the receiver relative to the RIS affects the quality of the reflected signal. However, finding the optimal position for the receiver may require some experimentation and testing. The complexity of the system is further increased if the receiver is moving. This can be simulated for example using the Poisson Point Process.

References

[1] ElMossallamy, M.A. *et al.* (2020) *Reconfigurable Intelligent Surfaces for Wireless Communications: Principles, Challenges, and Opportunities, IEEE Xplore*. IEEE. Available at: https://ieeexplore.ieee.org/abstract/document/9086766 (Accessed: April 5, 2023).

[2] Björnson, E. *et al.* (2022) *Reconfigurable Intelligent Surfaces: A signal processing perspective with wireless applications, IEEE Xplore*. Available at: https://ieeexplore.ieee.org/document/9721205 (Accessed: April 5, 2023).

[3] Barclay, L. (2013). *Propagation of Radiowaves.* The Institution of Engineering and Technology.

[4] Goldsmiths, A (2005). *Wireless Communications*. Cambridge University Press.

[5] Cho, Y.S. *et al.* (2010). *MIMO-OFDM Wireless Communication with MATLAB.* Wiley.

[6] Hanham, S. (2021) *Advanced Communication Systems Lecture 3*.

[7] Perovic, N.S. *et al.* (2021) *Achievable Rate Optimization for MIMO Systems with Reconfigurable Intelligent Surfaces*. Available at: https://arxiv.org/pdf/2008.09563.pdf (Accessed: April 5, 2023).

[8] Griffin, J.D. and Durgin, G.D. (2007) *Link Envelope Correlation in the Backscatter Channel, IEEE Xplore*. 10.1109/LCOMM.2007.070686. Available at: https://www.researchgate.net/publication/3418170_Link_Envelope_Correlation_in_the_Backscatter_Channel (Accessed: April 5, 2023).

[9] Wang, J. *et al.* (2021) *Interplay between RIS and AI in Wireless Communications: Fundamentals, Architectures, Applications, and Open Research Problems, ResearchGate*. Available at: https://www.researchgate.net/publication/348213253_Interplay_between_RIS_and_AI_in_Wireless_Communications_Fundamentals_Architectures_Applications_and_Open_Research_Problems (Accessed: April 5, 2023).

[10] Tang, W. *et al.* (2020) *Realization of Reconfigurable Intelligent Surface-Based Alamouti Space-Time Transmission*, *IEEE Xplore*. Available at: https://ieeexplore.ieee.org/document/9299726 (Accessed: April 5, 2023).

[11] Clerckx, B. (2014) *Advanced Wireless Communications*. Available at: http://www.ee.ic.ac.uk/bruno.clerckx/All%202014.pdf.

[12] Neumann, D., Wiese, T. and Utschick, W. (2018) *Learning the MMSE Channel Estimator*. IEEE. Available at: https://arxiv.org/pdf/1707.05674.pdf (Accessed: April 5, 2023).

[13] Liu, R. *et al.* (2021) *A Path to Smart Radio Environments: An Industrial Viewpoint on Reconfigurable Intelligent Surfaces*, *Arxiv*. Available at: https://arxiv.org/abs/2104.14985# (Accessed: April 5, 2023).

[14] Liu, Y. *et al.* (2021) *Reconfigurable Intelligent Surfaces: Principles and Opportunities*, *IEEE Xplore*. IEEE. Available at: https://ieeexplore.ieee.org/abstract/document/9424177 (Accessed: April 5, 2023).

[15] Kisseleff, S. *et al.* (2020) *Reconfigurable Intelligent Surfaces for Smart Cities: Research Challenges and Opportunities*, *IEEE Xplore*. Available at: https://ieeexplore.ieee.org/abstract/document/9253607 (Accessed: April 5, 2023).

[16] Williams, R.J., De Carvalho, E., and Marzetta, T.L. (2020) *A Communication Model for Large Intelligent Surfaces*, *Arxiv*. Available at: https://arxiv.org/pdf/1912.06644.pdf (Accessed: April 5, 2023).

[17] Bhowal, A. and Aïssa, S. (2022) *RIS-Aided Communications in Indoor and Outdoor Environments: Performance Analysis With a Realistic Channel Model*. IEEE. Available at: https://ieeexplore.ieee.org/document/9684924 (Accessed: April 5, 2023).

[18] Tran, V. (2020) *EVALUATION OF LDPC CODING TECHNIQUE TO OFDM SYSTEM IN AWGN AND MULTIPATH FADING CHANNEL USING MATLAB*. California State Polytechnic University, Pomona. Available at: https://scholarworks.calstate.edu/downloads/qr46r532k (Accessed: April 5, 2023).

[19] Sari, A. and Alzubi, A. (2018) *Path Loss Algorithms for Data Resilience in Wireless Body Area Networks for Healthcare Framework, ScienceDirect*. Academic Press. Available at: https://www.sciencedirect.com/science/article/pii/B9780128113738000136.

[20] Roberts, J.A. and Abeysinghe, J.R. (1995) *A two-state Rician model for predicting indoor wireless communication performance, IEEE Xplore*. IEEE. Available at: https://ieeexplore.ieee.org/document/525135 (Accessed: April 5, 2023).

[21] Carroll, M. and Wysocki, T.A. (2003) *Fading characteristics for indoor wireless channels at 5 GHz unlicensed bands, ResearchGate*. Available at: https://www.researchgate.net/publication/4046341_Fading_characteristics_for_indoor_wireless_channels_at_5_GHz_unlicensed_bands (Accessed: April 5, 2023).

[22] Sanchez, F., Stephanides, A. and Czink, N. (2011) *Fast Fading Characterization for Indoor to Indoor and Outdoor to Indoor Channels, IEEE Xplore*. IEEE. Available at: https://ieeexplore.ieee.org/document/6092969 (Accessed: April 5, 2023).

[23] Gulia, R. (2020) *Path Loss Model for 2.4GHZ Indoor Wireless Networks with Application to Drones*. Rochester Institute of Technology. Available at: https://scholarworks.rit.edu/cgi/viewcontent.cgi?article=11676&context=theses#:~:text=The%20ITU%20indoor%20propagation%20model,by%20walls%20of%20any%20form (Accessed: April 5, 2023).

[24] Weichselberger, W. *et al.* (2006) *A stochastic MIMO channel model with joint correlation of both link ends, IEEE Xplore*. IEEE. Available at: https://ieeexplore.ieee.org/document/1576533 (Accessed: April 5, 2023).

[25] Ma, Z. *et al.* (2021) *A Non-Stationary Geometry-Based MIMO Channel Model for Millimeter-Wave UAV Networks, IEEE Xplore*. IEEE. Available at: https://ieeexplore.ieee.org/document/9453775 (Accessed: April 5, 2023).

[26] Imoize, A.L. *et al.* (2021) *Standard Propagation Channel Models for MIMO Communication Systems, Hindawi*. Available at: https://www.hindawi.com/journals/wcmc/2021/8838792/ (Accessed: April 5, 2023).

[27] Riadi, A., BOULOUIRD, M. and Hassani, M.M. (2020) *Performances of OSIC Detector of an UpLink OFDM Massive-MIMO system in Rayleigh and Ricain fading channels*, *ResearchGate*. Springer. Available at: https://www.researchgate.net/publication/343350078_Performances_of_OSIC_Detector_of_an_UpLink_OFDM_Massive-MIMO_system_in_Rayleigh_and_Ricain_fading_channels (Accessed: April 5, 2023).

[28] Do, D.-T. *et al.* (2021) *Diversity and Multiplexing: A Fundamental Tradeoff in Multiple-Antenna Channels*, *ScienceDirect*. Available at: https://www.sciencedirect.com/science/article/abs/pii/S0167739X21003204?casa_token=BMMRdo259_QAAAAA:gWqix_rs9Afs6WLbj30nVtyekEW8TNm3WFH1dbljijNaYMnvicQ3FJjlBCyzK1bKL1TSSEkj5A (Accessed: April 5, 2023).

[29] Basar, E., Yildirim, I. and Kilinc, F. (2021) *Indoor and Outdoor Physical Channel Modeling and Efficient Positioning for Reconfigurable Intelligent Surfaces in mmWave Bands*, *IEEE Xplore*. IEEE. Available at: https://ieeexplore.ieee.org/document/9541182 (Accessed: April 5, 2023).

[30] Basar, E. and Yildirim, I. (2020) *SimRIS Channel Simulator for Reconfigurable Intelligent Surface-Empowered Communication Systems*, *Arxiv*. Available at: https://arxiv.org/pdf/2006.00468.pdf (Accessed: April 5, 2023).

[31] Basar, E. (2019) *Transmission Through Large Intelligent Surfaces: A New Frontier in Wireless Communications*, *Arxiv*. Available at: https://arxiv.org/pdf/1902.08463.pdf (Accessed: April 5, 2023).

[32] Basar, E. and Yildirim, I. (2021) *Reconfigurable Intelligent Surfaces for Future Wireless Networks: A Channel Modeling Perspective*, *IEEE Xplore*. IEEE. Available at: https://ieeexplore.ieee.org/document/9397266 (Accessed: April 5, 2023).

[33] Huang, Jie *et al.* (2022) *Reconfigurable Intelligent Surfaces: Channel Characterization and Modeling*, *Arxiv*. Available at: https://arxiv.org/pdf/2206.02308.pdf (Accessed: April 5, 2023).

[34] Basar, E. and Poor, H.V. (2021) *Present and Future of Reconfigurable Intelligent Surface-Empowered Communications*, *Arxiv*. Available at: https://arxiv.org/pdf/2105.00671.pdf (Accessed: April 5, 2023).

[35] Du, H. *et al.* (2020) *Millimeter Wave Communications With Reconfigurable Intelligent Surfaces: Performance Analysis and Optimization*, *Arxiv*. Available at: https://arxiv.org/pdf/2003.09090.pdf (Accessed: April 5, 2023).

[36] Sihlbom, B., Poulakis, M.I. and Di Renzo, M. (2021) *Reconfigurable Intelligent Surfaces: Performance Assessment Through a System-Level Simulator*, *Arxiv*. Available at: https://arxiv.org/pdf/2111.10791v1.pdf (Accessed: April 5, 2023).

[37] Ellingson, S. (2019) *Path Loss in Reconfigurable Intelligent Surface-Enabled Channels*, *Semantic Scholar*. Available at: https://www.semanticscholar.org/paper/Path-Loss-in-Reconfigurable-Intelligent-Channels-Ellingson/7f07dacac7627c8a7228ba909d69af1519358b78 (Accessed: April 5, 2023).

[38] Danufane, F.H. *et al.* (2021) *On the Path-Loss of Reconfigurable Intelligent Surfaces: An Approach Based on Green's Theorem Applied to Vector Fields*, *IEEE Xplore*. Available at: https://ieeexplore.ieee.org/document/9433568 (Accessed: April 5, 2023).

[39] Liu, F., Kwon, D.-H. and Tretyakov, S. (2022) *Reflectarrays and metasurface reflectors as diffraction gratings*, *Arxiv*. Available at: https://arxiv.org/pdf/2202.09029.pdf (Accessed: April 5, 2023).

[40] Budhu, J. and Grbic, A. (2020) *Perfectly Reflecting Metasurface Reflectarrays: Mutual Coupling Modeling Between Unique Elements Through Homogenization*, *IEEE Xplore*. Available at: https://ieeexplore.ieee.org/document/9119196 (Accessed: April 5, 2023).

[41] Li, B. *et al.* (2020) *Joint Array Diagnosis and Channel Estimation for RIS-Aided mmWave MIMO System*, *Semantic Scholar*. Available at: https://www.semanticscholar.org/paper/Joint-Array-Diagnosis-and-Channel-Estimation-for-Li-Zhang/01513bd5a31df36276a5388e323c8676d8ab1ac7 (Accessed: April 5, 2023).

[42] Kesir, S. et al.(2022) *Measurement-based Characterization of Physical Layer Security for RIS-assisted Wireless Systems*, *Arxiv*. Available at: https://arxiv.org/pdf/2212.07254v1.pdf (Accessed: April 5, 2023).

[43] Li, Y. *et al.* (2021) *Aerial Reconfigurable Intelligent Surface-Enabled URLLC UAV Systems*, *IEEE Xplore*. Available at: https://ieeexplore.ieee.org/stamp/stamp.jsp?tp=&arnumber=9567662 (Accessed: April 5, 2023).

[44] Björnson, E. and Sanguinetti, L. (2021) *Rayleigh Fading Modeling and Channel Hardening for Reconfigurable Intelligent Surfaces*, *Arxiv*. Available at: https://arxiv.org/pdf/2009.04723.pdf (Accessed: April 5, 2023).

[45] Papazafeiropoulos, A. *et al.* (2022) *Coverage Probability of STAR-RIS-Assisted Massive MIMO Systems With Correlation and Phase Errors*, *IEEE Xplore*. Available at: https://ieeexplore.ieee.org/stamp/stamp.jsp?tp=&arnumber=9786058 (Accessed: April 5, 2023).

[46] Yu, S. (2006) *Comparative Study of MIMO Systems with Linear Detection and Error-correction Code*, *Columbia University*. Available at: http://www.cisl.columbia.edu/grads/shihan/termpapers/EE6909syu.pdf (Accessed: April 5, 2023).

APPENDIX A

Revised Gantt Chart

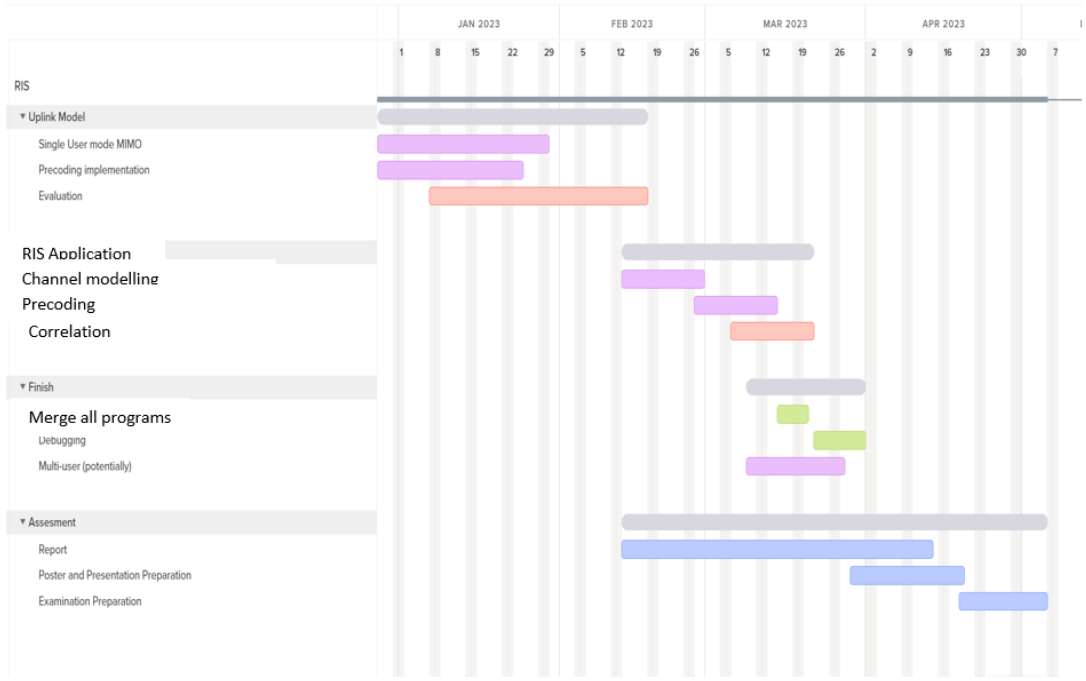

APPENDIX B

Original Gantt Chart

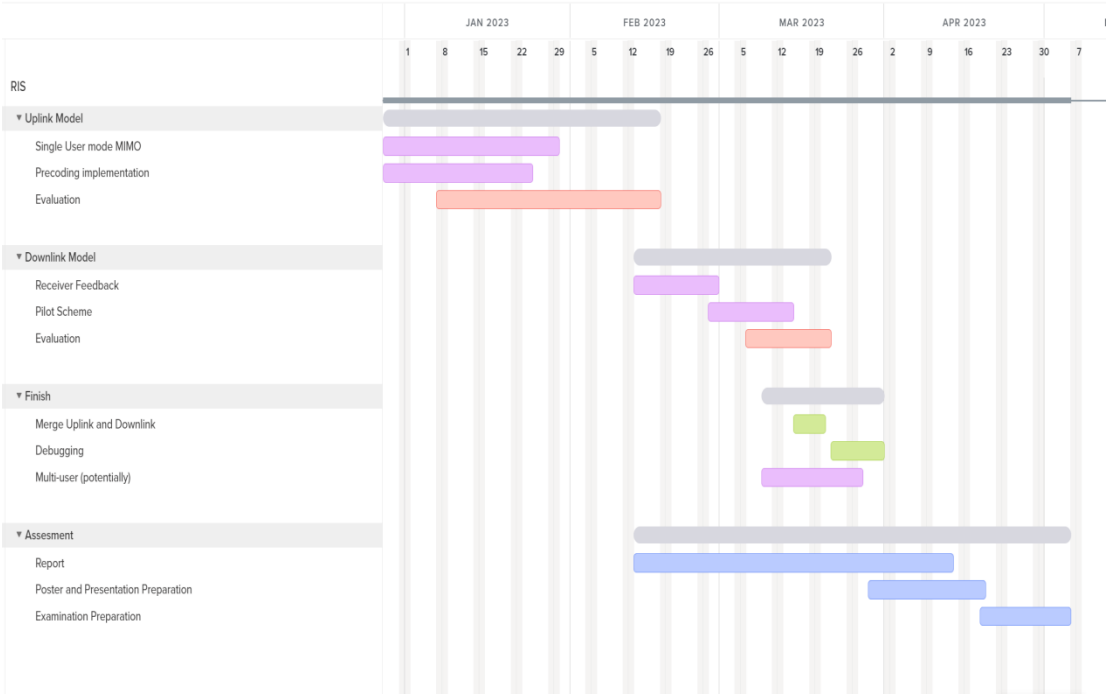

APPENDIX C

Channel Generation

```
function g = channel_ris(nr, nt, nris, z_imp)
H = randn(nris,nt) + 1j*randn(nris,nt); %tx-ris channel NLOS
h = randn(nr,nris) + 1j*randn(nr,nris); %ris-rx channel
d = randn(nr,nt) + 1j*randn(nr,nt); %tx-rx channel

phi = rand(nris, 1) * 2 * pi;
PHI = diag(exp(1j * phi),*z_imp');
g = h*PHI*H+d; %overall channel
end
```

APPENDIX D

Multi-User

```
clc
clear


% Signal Parameters
m = 4; %input('Enter Modulation Order: '); % Modulation order - VARIABLE!!!
k = log2(m); % Bits per Symbol
snr = 0:20; % SNR vector - !
fc = 2.4e9; % Carrier frequency [Hz] - VARIABLE!!
lambda = 3e8/fc; % Wavelength
k_w = (2*pi)/lambda; % Wavenumber
n_sym = 1000; % number of test symbols - !
ts = 1e-5; % Symbol period - VARIABLE!
r_sym = 1/ts; % Symbol rate
b = r_sym*k; % Signal bandwidth


% Ask for number of users
n_users = 2;% input('Enter number of users: ');


% Antenna Layout and Parameters
p_in = 1; % Input Power [W] - !
n_t = 4; %input('Enter Number of Transmitter Antenna elements: '); % Number of
transmitter antennas
n_r = 4; %input('Enter Number of Receiver Antenna elements: '); % Number of
receiver antennas
da = 0.5*lambda; % Antenna spacing


antpuser = n_r/n_users;
for ntr = 1:n_t
    z_tr = (ntr-1)*da;
    tx_pos(ntr,:) = [30 10 5+z_tr];
end
for user_no = 1:n_users


    for nre = 1:antpuser
        z_re = (nre-1)*da;
        rx_pos{user_no}(nre,:) = [-30 -10 -5+z_re];
    end
```

```
end


%RIS Dimensions
n_rows = 4;
n_columns = 4;


n_ris = n_rows*n_columns;
dris = 0.5*lambda;
% RIS Position
ris_pos = zeros(n_ris,3); % Cause 3D
idx = 1;
for row = 1:n_rows
    for col = 1:n_columns
        y = (col-1)*dris;
        z = (row-1)*dris;
        ris_pos(idx,:) = [0,y,z];
        idx = idx + 1;
    end
end


for user_no = 1:n_users
    for ris_no = 1:n_ris
        for rx_no = 1:n_r
            dist_risue{user_no}(ris_no,rx_no) = norm((rx_pos{user_no}(n_r)-
ris_pos(ris_no,:))); % Euclidean distance between the user andthe n-th RIS
element
            for rxchan = 1:size(rx_pos{user_no},1)
            v{user_no}(ris_no,rx_no) =
acos(rx_pos{user_no}(rxchan,1)/dist_risue{user_no}(ris_no,rx_no)); % Angle of
departure
            end
        end
        for tx_no = 1:n_t
            dist_txris(ris_no,tx_no) = norm(ris_pos(ris_no,:)-tx_pos(n_r));
        end
        dist_ris(ris_no) = norm((ris_pos(ris_no,:)-(-0.1)));
        z_imp(ris_no) = (sinc(k_w*(dist_ris(ris_no)-dist_ris(1))));
    end
end


% Path loss Calculation
for user_no = 1:n_users
    dist_tot{user_no} = dist_txris+dist_risue{user_no};
```

```
    p_l{user_no} = p_in*(((lambda/4)^2)./(4*pi*dist_tot{user_no}.^2));
end

%init
len = length(snr);
ber_mu = zeros(1,len);


for i = 1:len
    snr_value = 10.^(snr(i)/10);
    ea = 1; % Transmitter element power
    es = ea*n_t; % Total transmitted power
    sigma_n = es/snr_value; % noise power
    for user_no = 1:n_users
           %H{user_no} = sqrt(0.5)*randn(n_r,n_t)+1j*randn(n_r,n_t);
           H{user_no} = channel_ris(n_r/antpuser,n_t,n_ris,z_imp);
    end
    [U1,S1,V1] = svd(H{1});
    W2 = V1(:,3:4);
    [U2,S2,V2] = svd(H{2});
    W1 = V2(:,3:4);
    for sym_index = 1:n_sym
        tx_data = randi([0 m-1],n_r,1);
        tx_sig = pskmod(tx_data,m);


        n = sqrt(sigma_n/2)*(randn(n_r,2)+j*randn(n_r,2));


        tdata = W1*tx_sig(1:2)+W2*tx_sig(3:4);
       Rx1 = H{1}*tdata;
        Rx2 = H{2}*tdata;


        % Compute equalizers using block diagonalizing matrices
        W1_H1 = H{1}*W1;
        EQ1 = W1_H1'*inv(W1_H1*W1_H1');


        W2_H2 = H{2}*W2;
        EQ2 = W2_H2'*inv(W2_H2*W2_H2');


        % Equalize receivrd data and estimate symbols
        y = [EQ1*Rx1;EQ2*Rx2] + n;
```

```
        rx_data = pskdemod(y,m);
        [numerr errate] = biterr(rx_data,tx_data);

        ber_mu(1,i) = ber_mu(1,i)+errate(1);
    end
end
ber_mu_ris = ber_mu/n_sym;
```

APPENDIX E

7.2.2.1 Single-User

```
clear
clc
% System Parameters
m = 4; % Modulation order - VARIABLE!!!
k = log2(m); % Bits per Symbol
snr = 0:20; % SNR vector - !
fc = 2.4e9; % Carrier frequency [Hz] - VARIABLE!!
lambda = 3e8/fc; % Wavelength
k_w = (2*pi)/lambda; % Wavenumber
n_sym = 100000; % number of test symbols - !
ts = 1e-5; % Symbol period - VARIABLE!
r_sym = 1/ts; % Symbol rate
b = r_sym*k; % Signal bandwidth


% Antenna Layout and Parameters
p_in = 1; % Input Power [W] - !
n_t = 4; % Number of transmitter antennas
n_r = 4; % Number of receiver antennas
da = 0.5*lambda; % Antenna spacing


for ntr = 1:n_t
    z_tr = (ntr-1)*da;
    tx_pos(ntr,:) = [58 10 5+z_tr];
end


for nre = 1:n_r
    z_re = (nre-1)*da;
    rx_pos(nre,:) = [-30 -10 -5+z_re];
end
%RIS Dimensions
n_rows = 4;
n_columns = 4;


nris = n_rows*n_columns;
dris = 0.5*lambda;
% RIS Position
ris_pos = zeros(nris,3); % Cause 3D
idx = 1;
for row = 1:n_rows
    for col = 1:n_columns
        y = (col-1)*dris;
        z = (row-1)*dris;
        ris_pos(idx,:) = [0,y,z];
        idx = idx + 1;
```

```
    end
end
for ris_no = 1:nris
    for rx_no = 1:n_r
        dist_risue(ris_no,rx_no) = norm((rx_pos(n_r)-ris_pos(ris_no,:))); %
Euclidean distance between the user andthe n-th RIS element
        v(ris_no,rx_no) = acos(rx_pos(rx_no,1)/dist_risue(ris_no,rx_no)); %
Angle of departure
    end
    for tx_no = 1:n_t
        dist_txris(ris_no,tx_no) = norm(ris_pos(ris_no,:)-tx_pos(n_r));
    end
    dist_ris(ris_no) = norm((ris_pos(ris_no,:)-(-0.1)));
    z_imp(ris_no) = (sinc(k_w*(dist_ris(ris_no)-dist_ris(1))));
end


% Correlation (impedance) matrix
z_grid = reshape(z_imp,n_rows,n_columns);
%
%
% path loss calculation
dist_tot = dist_txris+dist_risue;
p_l = p_in*(((lambda/4)^2)./((4*pi)*dist_tot.^2));


%init
len = length(snr);
ber = zeros(1,len);


% Simulation


for i = 1:len
    snr_value = 10.^(snr(i)/10);
    ea = 1; % Transmitter element power
    es = ea*n_t; % Total transmitted power
    sigma_n = es/snr_value; % noise power


    threshold_snr = 15; %Snr threshold in dB
    p_sig = 0;

        rng(2,"twister")
        H = sqrt(0.5)*(randn(n_r,n_t)+1j*randn(n_r,n_t)); % Rayleigh MIMO
channel
        %H = channel_ris(n_r,n_t,nris,z_imp'); %RIS channel
        ZF_F = H'*inv(H*H'); %Precoding Matrix
        beta_zf = sqrt(es/norm(ZF_F,"fro").^2);
        F_ZF = beta_zf*ZF_F; %Normalized Precoding Matrix
        num_outages(i) = 0;
```

```
        for sym_index = 1:n_sym
            tx_data = randi([0 m-1],n_t,1); % data generation
            tx_sig = pskmod(tx_data,4); % Modulation
            tx_zf = F_ZF*tx_sig; % Precoding
            n = sqrt(sigma_n/2)*(randn(n_r,2)+j*randn(n_r,2)); %Noise
            y_zf = H*tx_zf+n(:,2);
            r_zf = 1/beta_zf*y_zf; %Received signal
            rec_data_zf = pskdemod(r_zf,m); % Received data
            [err ratio] = biterr(rec_data_zf,tx_data); %BER
            ber(1,i) = ber(1,i)+ratio;
            p_sig = p_sig + norm(F_ZF)^2; % Received signal power
            p_n = p_sig/(10^(snr(i)/10)); %Noise power
            received_snr(i) = (mean(mean(abs(H*es).^2/p_n))); %Received SNR
            received_snr_db = 10*log10((mean(mean(abs(H*es).^2/p_n))));
            if received_snr_db< 10
                 num_outages = num_outages +1;
            end
            r(i) = b*log2(1+received_snr(i)); %Data rate
        end
end
ber=ber/n_sym;
p_o_mimo = num_outages/(n_sym*len); %Outage Probability
```

APPENDIX F

University of Kent | Division of Computing, Engineering and Mathematical Sciences

RISK ASSESSMENT FORM

EDA RISK ASSESSMENT FORM

Overview of Activity: Mr Le is carrying out an engineering project "Deployment of Reconfigurable Intelligent Surfaces" under supervision of Dr H Zhu. This project aims to evaluate performance improvements of a communication channel when assisted by Reconfigurable Intelligent Surfaces.

Name: Huy Viet Le (hvl3)

Supervisor\Line Manager: Doctor H Zhu

Start date of activity: 05/10/2022

Location of your activity: Engineering Lab; Cornwallis; Jennison; Sibson

General activity type: Project (Student)

Pending approval

Activity Description

Additional Activities - Activities not yet in the list

Data Loss

Additional - Being a software-based project requiring mainly programming and research skills, the project involves low risk activities with the most serious risks arising from excessive eye contact with computer displays.

Activity: Data Loss								
Hazard	**Likelihood** (Chance of something happening)			**Consequence** (Impact of event happening)			**Who the hazard affects**	**Reduction of risk**
	Unlikely	Likely	Definite	Low	Moderate	High		
Data loss / corruption due to different causes		X			X		The student	Backup the work in as many ways as possible (USB drives, external drives, CD/DVD, cloud, etc.)
Activity: Additional Hazards								
Hazard	**Likelihood** (Chance of something happening)			**Consequence** (Impact of event happening)			**Who the hazard affects**	**Reduction of risk**
	Unlikely	Likely	Definite	Low	Moderate	High		
Prolonged Computer Use			X		X		The student	Work in well-lid spaces, take brakes regularly
Prolonged Computer Use			X		X		The student	Work in well-lid spaces, take brakes regularly
COVID-19	X			X			The student	Always make sure to have all the working software and files available on a personal computer